Neuron

Article

A direct lateral entorhinal cortex to hippocampal CA2 circuit conveys social information required for social memory

Highlights

- Lateral entorhinal cortex (LEC) inputs to hippocampal CA2 underlie social memory
- Medial entorhinal cortex (MEC) CA2 input is weak and not involved in social memory
- Social memory requires the direct but not indirect LEC inputs to CA2
- LEC CA2 inputs are selectively activated by social over non-social exploration

Authors

Jeffrey Lopez-Rojas, Christopher A. de Solis, Felix Leroy, Eric R. Kandel, Steven A. Siegelbaum

Correspondence

jl5545@columbia.edu (J.L.-R.), sas8@columbia.edu (S.A.S.)

In brief

Although the CA2 hippocampal region is essential for social memory and detection of social novelty, the inputs that provide social information to CA2 are unknown. We found that social memory depends on the direct inputs CA2 receives from the lateral entorhinal cortex. As this input is activated similarly by novel and familiar individuals, CA2 itself may compute novelty.

Lopez-Rojas et al., 2022, Neuron *110*, 1–14
May 4, 2022
https://doi.org/10.1016/j.neuron.2022.01.028

CellPress

Neuron

CellPress
OPEN ACCESS

Article

A direct lateral entorhinal cortex to hippocampal CA2 circuit conveys social information required for social memory

Jeffrey Lopez-Rojas,[1,4,*] Christopher A. de Solis,[1] Felix Leroy,[1,2] Eric R. Kandel,[1,3] and Steven A. Siegelbaum[1,*]
[1]Department of Neuroscience, The Kavli Institute for Brain Science, Mortimer B. Zuckerman Mind Brain Behavior Institute, Vagelos College of Physicians and Surgeons, Columbia University, New York, NY 10027, USA
[2]Instituto de Neurociencias CSIC-UMH, San Juan de Alicante, Spain
[3]Howard Hughes Medical Institute, Columbia University, New York, NY, USA
[4]Lead contact
*Correspondence: jl5545@columbia.edu (J.L.-R.), sas8@columbia.edu (S.A.S.)
https://doi.org/10.1016/j.neuron.2022.01.028

SUMMARY

The hippocampus is essential for different forms of declarative memory, including social memory, the ability to recognize and remember a conspecific. Although recent studies identify the importance of the dorsal CA2 region of the hippocampus in social memory storage, little is known about its sources of social information. Because CA2, like other hippocampal regions, receives its major source of spatial and non-spatial information from the medial and lateral subdivisions of entorhinal cortex (MEC and LEC), respectively, we investigated the importance of these inputs for social memory. Whereas MEC inputs to CA2 are dispensable, the direct inputs to CA2 from LEC are both selectively activated during social exploration and required for social memory. This selective behavioral role of LEC is reflected in the stronger excitatory drive it provides to CA2 compared with MEC. Thus, a direct LEC → CA2 circuit is tuned to convey social information that is critical for social memory.

INTRODUCTION

Memory formation depends on our ability to detect and distinguish novel from familiar sensory information and then to store that information in long-term memory. The hippocampus, which is classically known for its role in declarative memory, our repository of information of places, objects, events, and other individuals, has been found to be important for both novelty detection and long-term memory storage (Fernández and Morris, 2018; Kafkas and Montaldi, 2018; Strange et al., 2014). However, the neural circuits by which the hippocampus detects novelty and stores detailed information remain unknown. In particular, it is unclear whether these two functions are mediated by the same or distinct circuits. Here, we address this question by examining the neural circuitry responsible for hippocampal-dependent social novelty recognition and social memory, the ability of an animal to recognize and remember another of its species.

Recently, the CA2 subregion of the dorsal hippocampus has emerged as a critical element of a brain network supporting social recognition memory (Alexander et al., 2016; Donegan et al., 2020; Hitti and Siegelbaum, 2014; Meira et al., 2018; Middleton and McHugh, 2020; Oliva et al., 2020; Watarai et al., 2021). Although CA2 encodes both social novelty and social identity, the neural circuits that provide these social signals to CA2 are not well understood. One recent study reported that subcortical input to CA2 from the supramammillary nucleus provides information about social novelty (Chen et al., 2020). However, it is not known whether this input responds differentially to novel versus familiar conspecifics. Moreover, as the supramammillary nucleus inputs largely target inhibitory neurons in CA2 (Chen et al., 2020), it is unclear how this might enhance CA2 firing.

In contrast to the net inhibitory influence of the supramammillary nucleus, CA2, like other hippocampal regions, receives its major excitatory input from the entorhinal cortex (EC). This multimodal association area conveys spatial and non-spatial sensory information to hippocampus through its medial (MEC [medial entorhinal cortex])—which contains spatially tuned grid cells, head-direction cells, and border cells (Moser et al., 2014)—and lateral (LEC [lateral entorhinal cortex]) subdivisions, respectively (Connor and Knierim, 2017; Eichenbaum et al., 2007; Reagh and Yassa, 2014). Information from MEC and LEC reaches CA1 and CA2 regions through parallel indirect and direct pathways. In the indirect, or trisynaptic, route, EC sends excitatory input through the perforant path to the dentate gyrus (DG), whose mossy fibers strongly excite CA3 pyramidal neurons (PNs) and weakly excite CA2 PNs. In the classic trisynaptic path, the Schaffer collateral projections of CA3 PNs strongly excite CA1 PNs, which provide the major output of hippocampus. Although the Schaffer collaterals also excite CA2 PNs, this second trisynaptic path is dominated by strong feedforward inhibition (Chevaleyre and Siegelbaum, 2010). In addition to these indirect routes, EC sends direct input that strongly excites CA2 PNs

Please cite this article in press as: Lopez-Rojas et al., A direct lateral entorhinal cortex to hippocampal CA2 circuit conveys social information required for social memory, Neuron (2022), https://doi.org/10.1016/j.neuron.2022.01.028

but only weakly excites CA1 and CA3 PNs (Chevaleyre and Siegelbaum, 2010; Sun et al., 2014). As CA2 PNs powerfully excite CA1 PNs, the EC → CA2 → CA1 circuit provides a disynaptic pathway linking EC input to CA1 output.

To date, the relative importance for social memory of the direct versus indirect routes by which information from EC arrives in CA2 is unknown. Moreover, it is not clear whether LEC or MEC inputs are specifically involved in social memory. Finally, we do not know whether these inputs selectively participate in social novelty detection or social memory storage. Here, we use an optogenetic approach to dissect the relative strength of the direct MEC and LEC inputs in exciting CA2 PNs of young adult male mice. We then compare the roles of the direct MEC and LEC inputs to CA2 with the indirect inputs that arrive via DG in mediating social memory storage. Finally, we use fiber photometry to ask whether EC inputs to CA2 are activated during a social experience and whether they differentially respond to a novel compared with a familiar animal. Our results indicate that the direct LEC inputs, but not the MEC inputs, are activated during social interaction and provide a strong excitatory drive to CA2 that is required for social memory storage.

RESULTS

Strong dorsal CA2 depolarization by the lateral entorhinal cortex

As a first step in exploring how social information is conveyed to CA2, we examined the relative contributions of its direct inputs from MEC and LEC using patch clamp recordings from CA2 PNs in acute slices from dorsal hippocampus. Electrical stimulation of MEC and LEC axons with an electrode in the stratum lacunosum moleculare (SLM), the site of the direct inputs, evoked a large postsynaptic potential (PSP) in CA2 PNs (Figures S1A and S1B), as previously reported (Chevaleyre and Siegelbaum, 2010; Srinivas et al., 2017; Sun et al., 2014).

To investigate the differential contribution of the EC regions to the activation of dorsal CA2 neurons, we took advantage of the spatial segregation of the MEC and LEC fiber pathways as they traverse, respectively, the middle and outer molecular layers of DG en route to CA2. The PSP recorded in CA2 PNs evoked by stimulating the LEC pathway was around 1.5- to 2.0-fold larger than the PSP evoked by MEC stimulation (Figures S1C–S1E). We observed a similar differential response in the size of the extracellular field excitatory postsynaptic potential (fEPSP) recorded in the SLM of CA2 (Figure S2).

To obtain more direct evidence for a preferential role of LEC in exciting CA2 PNs, we used an optogenetic approach to selectively activate MEC or LEC inputs (Figure 1A). Because CA2 receives its direct EC input from the stellate and fan cell neurons in layer 2a of EC (Fujimaru and Kosaka, 1996; Leitner et al., 2016), we injected an adeno-associated virus (AAV) in the superficial layers of MEC or LEC to express the excitatory light-activated channel channelrhodopsin2 (ChR2) in these cells. Patch clamp recordings from CA2 PNs in hippocampal slices revealed that optogenetic stimulation of these inputs evoked a large monosynaptic PSP when ChR2 was expressed in either LEC or MEC. However, similar to the results from electrical stimulation, a significantly greater response was evident with ChR2 expressed in LEC compared with MEC, with LEC-evoked PSPs roughly twice as large as MEC-evoked responses (Figures 1B and 1C). This difference was also present when trains of stimuli, rather than single pulses, were used (Figure 1D). Moreover, the difference between LEC- and MEC- evoked responses was mainly due to differences in excitatory transmission, as we observed a similar relative difference when we blocked inhibition with antagonists of $GABA_A$ and $GABA_B$ receptors to measure the pure excitatory postsynaptic potential (EPSP) (Figures S3A–S3E).

As a further measure of the relative influence of MEC and LEC inputs, we expressed the inhibitory opsin archaerhodopsin-T (Arch) in LEC or MEC and examined how selective inhibition of either pathway affected the PSP evoked by electrical stimulation in SLM. Illumination of the SLM with yellow light in slices from mice in which Arch was expressed in MEC or LEC significantly decreased the PSP evoked by electrical stimulation in SLM. However, the extent of inhibition of the PSP was significantly greater when Arch was expressed in LEC than when it was expressed in MEC (Figures S3F and S3G), supporting the view that the direct LEC input predominates over the MEC input in exciting CA2.

Anatomical support for a larger influence of LEC than MEC on CA2 excitation came from an examination of the pattern of these inputs when labeled with GFP-tagged ChR2. Consistent with their topology in DG (Steward, 1976), the two sets of fibers were differentially localized in CA2, with MEC axons localized to a narrow strip in a more proximal domain of SLM in CA2 (closer to the soma) compared with LEC, whose axons occupied a broader more distal region in SLM, extending to the border with DG. Moreover, the width of the LEC projection was ~2-fold larger than that of MEC, consistent with the relative synaptic weights of the two inputs (Figure S4). To gain a more direct measure as to the relative difference in the number of LEC and MEC neurons that project to CA2, we used monosynaptic retrograde tracing by injecting G-deleted rabies virus and Cre-dependent helper virus into the CA2 region of *Amigo2-Cre* mice, which express Cre relatively selectively in CA2 PNs. Retrogradely labeled cells were observed in both LEC and MEC, as previously described (Hitti and Siegelbaum, 2014; Kohara et al., 2014). However, the number of rabies$^+$ cells was significantly higher in LEC, roughly twice as great compared with the MEC (Figures 1D and 1E).

The above results provide a coherent picture showing that while both MEC and LEC strongly excite CA2 PNs through their direct projections in the dorsal hippocampus, activation of the LEC inputs evoked a PSP in CA2 PNs that is 1.5- to 2.0-fold larger than that evoked by MEC inputs. This difference can be accounted for by the roughly 2-fold greater number of LEC neurons that project to CA2 compared with MEC. Next, we asked whether these differences in synaptic strength were reflected in the behavioral influence of these two regions on CA2-dependent social memory.

Disrupting the lateral entorhinal input to dorsal CA2 impairs social memory

To investigate the role of the EC projections to dorsal CA2 in social memory, we expressed Arch or GFP in LEC or MEC and illuminated their projections in dorsal CA2 with yellow light as

Please cite this article in press as: Lopez-Rojas et al., A direct lateral entorhinal cortex to hippocampal CA2 circuit conveys social information required for social memory, Neuron (2022), https://doi.org/10.1016/j.neuron.2022.01.028

CellPress
OPEN ACCESS

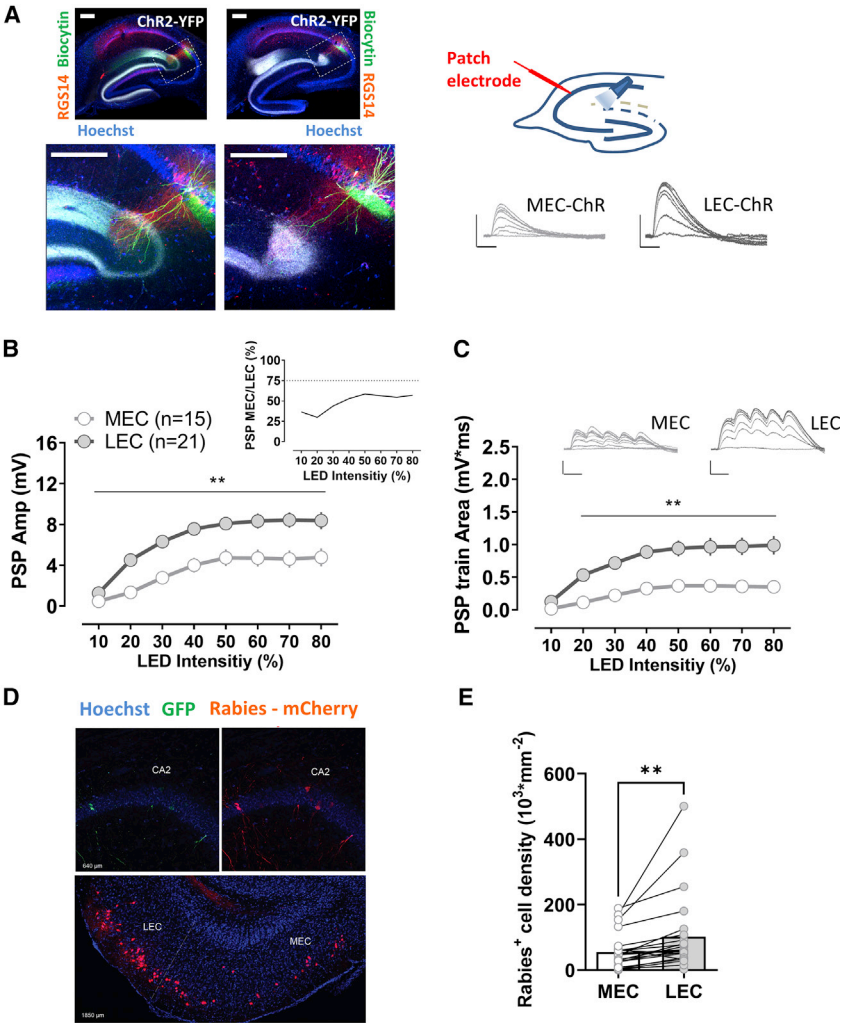

Figure 1. Comparison of synaptic responses of CA2 pyramidal neurons to their direct medial and lateral entorhinal cortical inputs

(A–C) (A) An AAV was injected to express ChR2 in the medial (MEC) or the lateral entorhinal cortex (LEC). Transverse hippocampal sections show MEC or LEC ChR2-YFP-labeled fibers, as well as biocytin-filled CA2 neurons and staining for the CA2 region marker RGS14 at low (upper panels) and high magnification (lower panels). Photostimulation of ChR2-expressing terminals in the stratum lacunosum moleculare evoked a large postsynaptic potential in CA2 pyramidal neurons in acute hippocampal slices for both MEC and LEC injected groups. The LEC-evoked response (21 cells from 21 slices from 7 animals) was significantly larger than the MEC-evoked response (15 cells from 15 slices from 5 animals) using either a single light pulse (B) or a short train of optical stimuli (C). $^{**}p < 0.01$ Holm-Sidak's post hoc test after two-way mixed-design ANOVA (B and C; in B, $F = 4.963$ $p < 0.0001$ for interaction stim LED intensity × PP M-L; in C, $F = 9.479$, $p < 0.0001$ for interaction stim LED intensity × PP M-L).

(D) Monosynaptic contacts to dorsal CA2 from the entorhinal area originate largely from the LEC. Retrograde tracing from dorsal CA2 using G-deleted rabies virus expressing mCherry (Rabies- mCherry), after CA2 infection with a Cre-dependent helper virus (expressing GFP). Coronal hippocampal sections in the upper panel and entorhinal horizontal slice in the lower panel.

(E) The number of mCherry-positive cells is greater in LEC than MEC (23 sections from 5 animals). $^{**}p < 0.01$, paired t test.

Scale bars: 5 mV/25 ms and 200 μm.

animals were engaged in an open arena, two-choice social memory task (Oliva et al., 2020). In the learning phase of this task, a subject mouse was allowed to explore for 5 min a square arena in which two novel stimulus mice (S1 and S2) were presented in wire cup cages in opposite corners of the arena. The subject mouse was then placed in its home cage for 30 min, after which a memory recall test was performed, in which the subject mouse explored for 5 min the same arena containing one of the two original stimulus mice and one completely novel mouse (N). Social memory was assessed by the preference of the subject mouse to explore the novel mouse (N) compared with the original, now-familiar stimulus mouse (S1 or S2). We quantified this preference with a discrimination index (DI) = (time exploring mouse N − time exploring mouse S)/(time exploring mouse N + time exploring mouse S).

We first examined the effects of silencing the LEC inputs to CA2 (Figure 2A). As expected, control mice expressing GFP in LEC spent significantly more time interacting with a novel animal compared with the now-familiar mouse in the memory recall trial (Figures 2B and 2F). As a second index of social memory, we found that control mice habituated to the stimulus mouse encountered during the learning trial, measured by the reduced time spent exploring the stimulus mouse in the recall trial compared with the time spent exploring the same mouse during the learning trial (Figures 2D and 2H). Illumination of the CA2 region with yellow light during either the learning or recall trials did not affect memory performance in the control group (Figure 2). In contrast, in mice expressing Arch in LEC, silencing of dorsal CA2 by illumination with yellow light during either the learning or recall trial produced a significant impairment in social memory performance, based on the similar amount of time such mice spent exploring the novel and now-familiar mouse during the recall trial (Figures 2B and 2F). Consistent with a reduction in social recognition memory, optogenetic silencing of CA2 reduced the normal habituation to the stimulus mouse when it was reintroduced in the recall trial (Figures 2D and 2H).

In contrast to the deficits in social memory observed when the LEC inputs to CA2 were silenced, optogenetic silencing of the MEC inputs to CA2 did not inhibit social memory, either when illumination was applied during the learning or recall trial (Figure 3). Thus, mice expressing Arch in MEC showed a normal preference for the novel animal in the recall trial, regardless of whether light was applied during the learning or recall trial. Moreover, illumination of CA2 of

Please cite this article in press as: Lopez-Rojas et al., A direct lateral entorhinal cortex to hippocampal CA2 circuit conveys social information required for social memory, Neuron (2022), https://doi.org/10.1016/j.neuron.2022.01.028

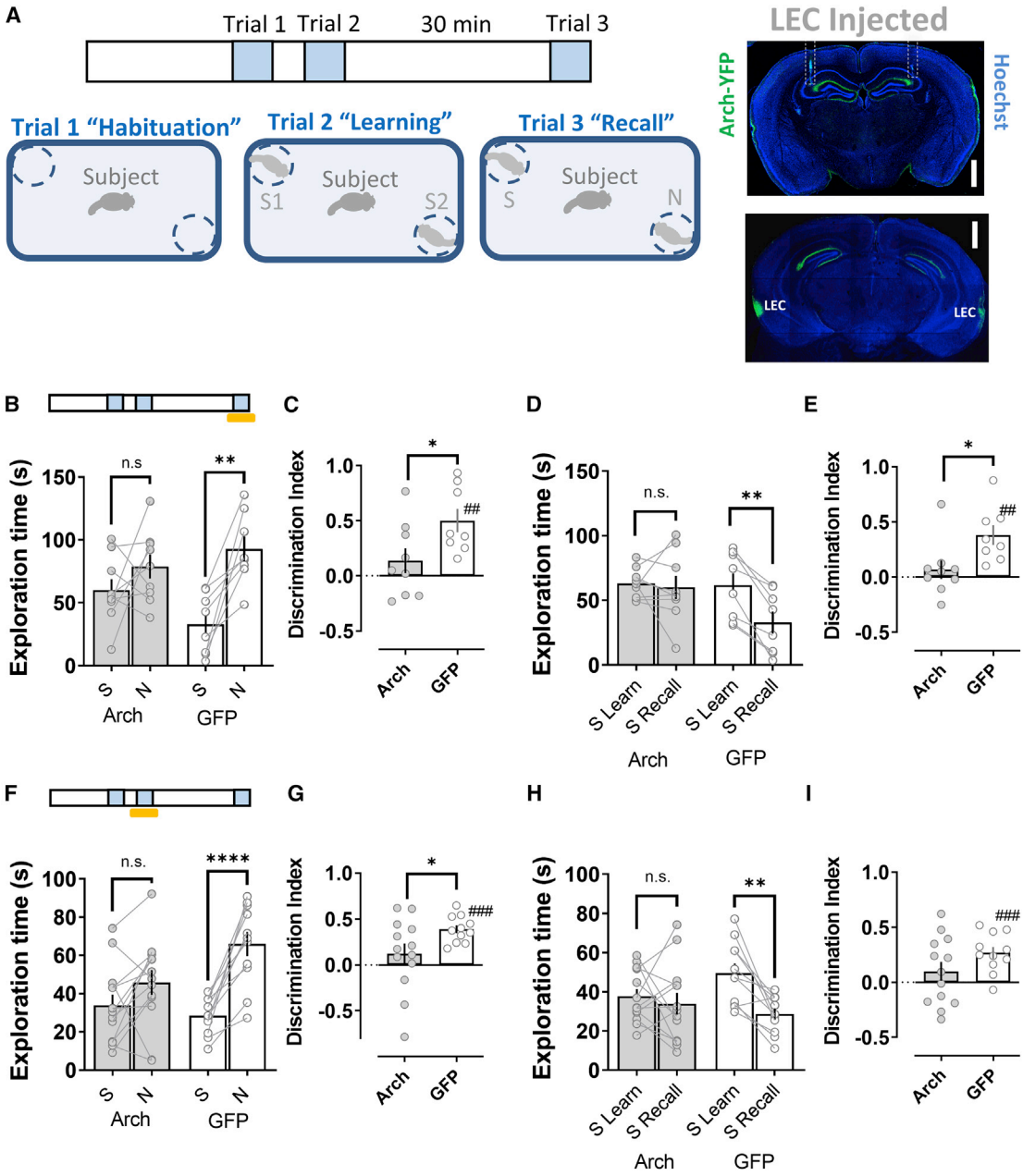

Figure 2. Disrupting the lateral entorhinal cortical input to dorsal CA2 impairs social memory

(A–I) (A) Schema of the two-choice social memory task consisting of three trials. Mice first explored the arena with two empty cups (trial 1 habituation). Next, two novel stimulus mice (S1 and S2) were placed one in each cup; the subject mouse was allowed to explore the arena with the two novel mice for 5 min in trial 2 (learning). The subject mouse was then removed from the arena for a 30-min inter-trial interval, after which it was reintroduced to the arena in a 5 min recall trial (trial 3), in which one of the stimulus mice presented in trial 2 (S1 or S2) was replaced by a third novel mouse (N). Social memory is manifest as (1) a greater time spent exploring mouse N compared with the now-familiar stimulus mouse (S1 or S2) in the recall trial (B and F) as quantified by a discrimination index (C and G) and (2) a decreased time spent exploring S1 or S2 in the recall trial relative to the learning trial (D and H) as quantified by a discrimination index (E and I). Insets show the expression of Arch in the lateral perforant path and the optical fiber location (dashed outline) in a coronal brain slice from a mouse previously injected in lateral entorhinal cortex (LEC) with an Arch-expressing AAV. Shining yellow light on LEC inputs in dorsal CA2 during the recall phase of the task (trial 3, Arch n = 9, GFP n = 8) (B–E) or during the learning phase (trial 2, Arch n = 13, GFP n = 11) (F–I), impairs social memory performance of animals expressing Arch in LEC relative to the control group expressing GFP. Scale bar: 1 mm. *$p < 0.05$ t test. ##$p < 0.01$, ###$p < 0.001$ one-sample t test against "0." **$p < 0.01$, ****$p < 0.0001$ Holm-Sidak's post hoc test after two-way mixed-design ANOVA (in B, $F = 4.912$ $p < 0.0001$ for interaction familiarity × genotype; in D, $F = 6.778$ $p = 0.0200$ for interaction familiar L-R × genotype; in F, $F = 8.357$ $p = 0.0085$ for interaction familiarity × genotype; in H, $F = 4.611$ $p = 0.0430$ for interaction familiar L-R × genotype).

Please cite this article in press as: Lopez-Rojas et al., A direct lateral entorhinal cortex to hippocampal CA2 circuit conveys social information required for social memory, Neuron (2022), https://doi.org/10.1016/j.neuron.2022.01.028

CellPress
OPEN ACCESS

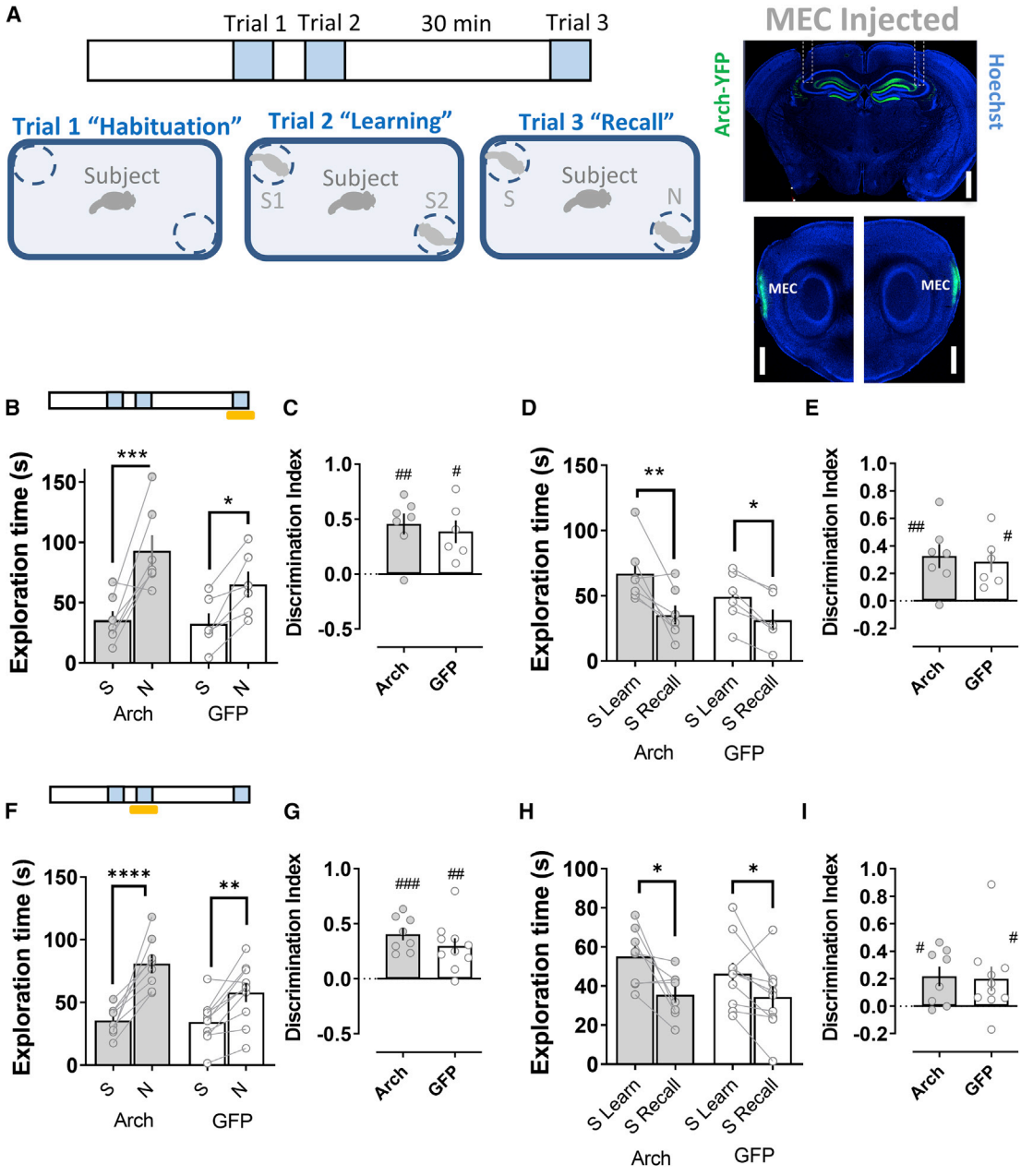

Figure 3. Disrupting the medial entorhinal cortical input to dorsal CA2 does not affect social memory

(A) Schema of the social memory task described in Figure 2. Insets show the expression of Arch in the medial perforant path and medial entorhinal cortex (MEC) in a coronal brain slice (upper panel) and in sagittal brain slices (lower panel) from a mouse previously injected in the MEC with an Arch-expressing AAV. Scale bar: 1 mm.

(A–I) Shining yellow light on MEC inputs in dorsal CA2 during the recall phase of the task (trial 3, Arch n = 7, GFP n = 6) (B–E) or during the learning phase (trial 2, Arch n = 8, GFP n = 10) (F–I) does not impair social memory in mice expressing Arch in MEC relative to the control group expressing GFP. #p < 0.05, ##p < 0.01, ###p < 0.001 one-sample t test against "0." *p < 0.05, **p < 0.01, ***p < 0.001, ****p < 0.0001 Holm-Sidak's post hoc test after two-way mixed-design ANOVA (in B, F = 30.04 p = 0.0002 for familiarity; in D, F = 22.90 p = 0.0006 for familiar L-R; in F, F = 5.145 p = 0.0375 for interaction familiarity × genotype; in H, F = 14.49 p = 0.0015 for familiar L-R).

Arch-expressing mice did not prevent the normal habituation to the stimulus mouse.

The social memory deficits seen with optogenetic silencing of the LEC inputs to CA2 were not attributable to a general impairment of novelty detection as optogenetic silencing of LEC terminals in CA2 did not affect performance in a novel object recognition test, using a paradigm similar to our social memory test (Figures S5A–S5C). Moreover, the lack of social recognition,

which requires recognition of olfactory cues, was not due to a general impairment in olfaction as optogenetic silencing of either LEC or MEC inputs to CA2 did not impair an animal's ability to find a hidden food pellet (Figure S5D). Thus, our data suggest that the information that LEC, but not MEC, provides to CA2 plays a specific role in social novelty discrimination.

To explore the generality of our behavioral results, we investigated how disrupting the communication between LEC or MEC and dorsal CA2 affected social recognition in a different behavioral paradigm, the direct interaction task (Figures S6 and S7). In this task, subject mice freely explored a novel juvenile male stimulus mouse for 2 min during a learning trial. The stimulus mouse was then removed from the arena and after a 30-min inter-trial interval it was reintroduced into the test arena for a recall trial. In this task, social memory is manifest as a habituation to the stimulus mouse, based on the reduction in social exploration time during the recall trial compared with the learning trial. Control mice expressing GFP in LEC terminals showed a significant reduction in exploration time when the same juvenile was reintroduced in the recall trial, independently of whether dorsal CA2 was illuminated with yellow light during the learning or recall trials. In contrast, mice expressing Arch in LEC that were illuminated with yellow light during either the learning or recall trials failed to show a decrease in the exploration of the juvenile in the recall trial (Figure S6). Optogenetic silencing of MEC inputs to CA2 during either the learning or recall trials caused no impairment in social memory (Figure S7). Next, we performed a control experiment to determine if the decreased exploration time during the recall trial resulted from fatigue of the subject mice or lack of motivation for social exploration, rather than a memory-specific habituation to the stimulus mouse. In this experiment, rather than exposing a mouse to the same novel animal in both trials, we introduced a second novel juvenile mouse during the recall trial. In all experimental groups, subject mice explored the two novel mice to equal extents in the two trials, indicating that the decreased exploration of the familiar mouse in a recall trial did indeed represent a true habituation to the novel mouse due to social memory (Figure S8).

Information flow through the dorsal trisynaptic path is dispensable for social memory

Although our results above suggest that the direct inputs from LEC to CA2 are required for social memory, it is also possible that information conveyed through the trisynaptic path, from EC to DG to CA3 to CA2, or through a disynaptic path, from EC to DG to CA2 (Kohara et al., 2014), is also necessary. Furthermore, our approach using a fiber optic probe targeting EC axons in CA2 may have allowed sufficient light to reach the EC axons in dorsal DG, thereby inhibiting the activation of DG by its EC inputs. Thus, to explore any possible contribution of DG activation to the behavioral effects we observed with optogenetic silencing of the EC inputs in CA2, we directly examined the effect of silencing DG granule cells on social memory performance.

To ensure that we silenced as large a population of DG granule cells as possible, we used a pharmacogenetic approach, in which a DG granule cell Cre mouse line (*POMC-Cre*) (McHugh et al., 2007) was crossed with a mouse line expressing the inhibitory designer receptor exclusively activated by designer drug (DREADD) hM4Di under control of Cre (Zhu et al., 2016), enabling us to silence DG granule cells using injection of the DREADD ligand clozapine N-oxide (CNO). The efficacy of this approach is supported by the previous finding from our laboratory that DREADD-based silencing of CA2 PNs in the dorsal hippocampus markedly impaired social recognition memory (Meira et al., 2018). We further confirmed the efficacy of this approach for other cortico-hippocampal regions by showing that hM4Di expression in LEC and local infusion of CNO through a cannula to CA2 produced a robust inhibition of social memory (Figure S9), equivalent to that seen with optogenetic Arch-based inhibition of LEC. Finally, we confirmed that inhibitory DREADD expression in DG of POMC-Cre+ mice was effective in reducing granule cell activity by showing that CNO infusion to DG through a cannula 30 min before an i.p. injection of the convulsant pilocarpine greatly reduced the number of c-Fos$^+$ granule cells, compared with a Cre− control group infused with CNO prior to pilocarpine (Figure 4A).

In contrast to the ability of CNO to inhibit DG activity, infusion of the DREADD agonist into DG of mice 30 min prior to the two-choice social recognition test failed to impair social memory. Thus CNO-treated Cre+ mice and Cre− control animals both explored the novel mouse for a significantly greater time than the familiar mouse during the memory recall trial (Figures 4C and 4D). Furthermore, both groups of mice spent significantly less time exploring the now-familiar mouse in the recall trial than during the learning trial (Figures 4E and 4F). Our findings thus suggest that dorsal DG granule cells do not significantly contribute to social memory in mice, implying that it is indeed the direct LEC inputs to CA2 that are of key importance.

Input from the lateral entorhinal cortex to CA2 is selectively enhanced during social exploration

How does the LEC participate in social memory and what is the basis for its selective involvement in social memory relative to MEC? To gain insight into these questions we investigated whether LEC or MEC responds to socially relevant information by staining these regions for expression of the immediate-early gene c-Fos as a marker of neuronal activity following the recall phase of the two-choice social memory task. We observed a significant increase in the number of c-Fos$^+$ cells in both MEC and LEC following social exploration, relative to c-Fos$^+$ cells in mice kept in their home cage (Figure 5). Although the overall number of c-Fos$^+$ cells was similar in LEC and MEC, we observed a significantly greater number of c-Fos$^+$ cells in the superficial layers of LEC compared with the superficial layers of MEC ($p < 0.01$, paired t test). In addition, for LEC, the number of c-Fos$^+$ cells was significantly greater in superficial layers compared with deep layers of LEC ($p < 0.001$, paired t test). In contrast to LEC, the two layers contained similar numbers of c-Fos$^+$ cells in MEC. The preferential increase in c-Fos labeling of superficial LEC compared with superficial MEC is important since it is the superficial layers that contain the cells that project to CA2.

To determine whether the increase in c-Fos$^+$ cells was selective for exposure to social novelty, we examined mice that had performed a two-choice novel object recognition task, analogous to the social recognition task. Although we

Please cite this article in press as: Lopez-Rojas et al., A direct lateral entorhinal cortex to hippocampal CA2 circuit conveys social information required for social memory, Neuron (2022), https://doi.org/10.1016/j.neuron.2022.01.028

CellPress
OPEN ACCESS

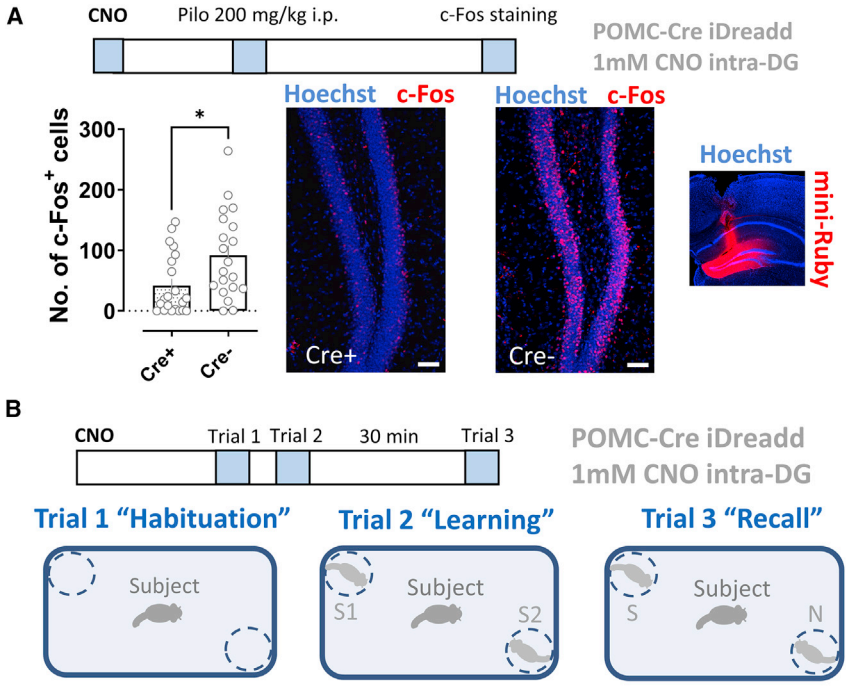

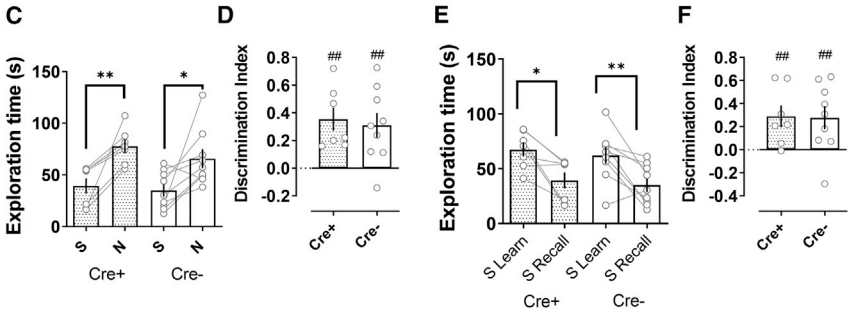

Figure 4. Pharmacogenetic silencing dorsal dentate gyrus granule cells does not impair social memory

(A) A pharmacogenetics approach effectively reduces dentate granule cell activity. The inhibitory DREADD (iDREADD) agonist CNO (1 mM, 1 μl per side) was infused into the dorsal dentate gyrus of *POMC-Cre+* × Rosa26-LSL-hM4Di-mCitrine (Cre+) mice expressing iDREADD in DG granule cells or control mice (*POMC-Cre-* × Rosa26-LSL-hM4Di-mCitrine, Cre−). After 30 min mice were given an i.p. injection of pilocarpine. CNO significantly reduced the number of c-Fos+ neurons in the iDreadd group (Cre+, 20 sections from 4 animals) compared with that of controls (Cre−, 21 sections from 4 animals). The inset to the right shows the spread of 1 μL of the dye mini-Ruby infused locally into the dorsal DG. Scale bar: 50 μm. *p < 0.05, t test.

(B) Schema of the social memory task.

(C–F) CNO injection into the dentate gyrus of iDreadd mice (Cre+, 7 animals) did not significantly impair social memory performance compared with the control group (Cre−, 9 animals). ##p < 0.01 one-sample t test against "0." *p < 0.05, **p < 0.01, Holm-Sidak's post hoc test after two-way mixed-design ANOVA (in C, F = 21.26 p = 0.0004 for familiarity; in E, F = 22.81 p = 0.0003 for familiar L-R).

found a significant increase in c-Fos$^+$ cells in MEC following exploration of a novel object, relative to animals in their home cage, there was no significant increase in c-Fos$^+$ cells in LEC (Figure 5). As a result, for LEC the number of c-Fos$^+$ superficial layer cells was significantly greater following social exploration compared with object exploration. In contrast, for MEC a similar number of c-Fos$^+$ superficial cells were found following social or object exploration. These results suggest that LEC is selectively tuned to respond to social signals relative to MEC, consistent with the greater behavioral importance of LEC for social memory.

Finally, we assessed the dynamics of LEC input activity in dorsal CA2 during social and object exploration by using targeted viral injections to express the genetically encoded fluorescent Ca^{2+} sensor GCaMP7f in LEC superficial neurons and fiber photometry to measure Ca^{2+} levels in LEC projections to CA2 (Figure 6A). Bouts of exploration of a novel conspecific elicited a large, consistent increase in GCaMP7f fluorescence. In contrast, object exploration produced a weak, non-significant increase in fluorescence, consistent with the c-Fos staining patterns observed above. We then performed Ca^{2+} signal measurements during social exploration of a familiar littermate, which elicited large increases in GCaMP7f fluorescence that were comparable with the levels seen during exploration of a novel animal (Figures 6B and 6C). This result suggests that whereas mean levels of LEC activity are significantly enhanced by social exploration, the mean activity elicited by novel compared with familiar animals does not differ.

To enable a more direct comparison of mean LEC activity to social memory behavior, we recorded Ca^{2+} signals from LEC inputs to CA2 as an animal performed the two-choice social memory test described above. We found that exploration of the various stimulus mice during both learning and recall trials produced significant increases in LEC activity (Figure 7A). However, we found no difference in the peak amplitude of the Ca^{2+} signals during exploration of the novel versus familiar mouse in the memory recall trial, despite the normal behavioral preference of the subject mouse for the novel animal (Figures 7B, 7C, and S10).

Next we examined whether LEC Ca^{2+} activity distinguishes a novel from familiar animal using a social habituation paradigm, which we previously found to depend on CA2 (Hitti and Siegelbaum, 2014). In this test, a subject mouse is allowed to explore the same, initially novel, stimulus mouse for four successive trials, followed by presentation of a novel mouse in trial 5 (Figure 7D). This elicits a progressive decrease in exploration (habituation) to the stimulus mouse in trials 1–4, followed by an increased exploration of the novel mouse in trial 5 (Figure 7E). Despite the behavioral changes, the Ca^{2+} activity of LEC inputs

Please cite this article in press as: Lopez-Rojas et al., A direct lateral entorhinal cortex to hippocampal CA2 circuit conveys social information required for social memory, Neuron (2022), https://doi.org/10.1016/j.neuron.2022.01.028

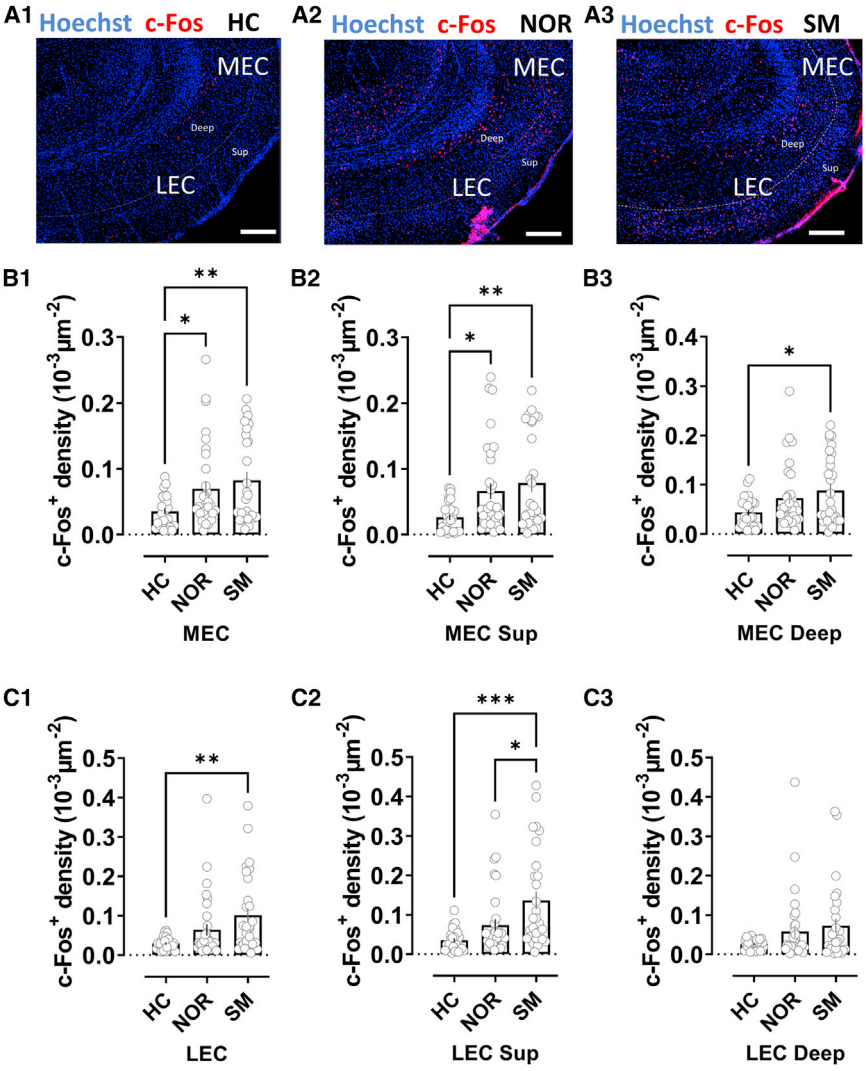

Figure 5. Social exploration preferentially activates lateral compared with medial entorhinal cortex

(A) Staining for c-Fos in lateral (LEC) and medial (MEC) entorinal cortices in horizontal brain slices from mice in control home-cage conditions (HC) or following novel object recognition (NOR) or social memory (SM) tasks.

(B) Quantification of c-Fos+ cell density in MEC in both deep and superficial layers combined (B1) or separated into superficial (B2) or deep layers (B3). Mice subjected to the NOR or SM task showed a significantly larger density of c-Fos+ cells than mice in HC conditions in both entire MEC and in superficial MEC layers. In deep MEC layers the increase over HC c-Fos+ staining was only significant following the SM task, although there was a trend in the NOR task. There was no significant difference in c-Fos+ density following SM compared with NOR task in total MEC (B1) or individual layers (B2 and B3).

(C) In superficial and deep LEC layers combined (C1) and superficial LEC layers alone (C2), we observed a significant increase in c-Fos+ density compared with HC levels following the SM task, with no significant increase following the NOR task (although there was a trend). We saw no significant change in either SM or NOR tasks in deep LEC alone (C3). c-Fos+ density in superficial LEC was significantly greater following SM task compared with NOR task. HC, 27 sections from 4 animals; NOR, 32 sections from 4 animals; SM, 29 sections from 4 animals.

Scale bar: 200 µm. *p < 0.05, **p < 0.01, ***p < 0.001 Holm-Sidak's post hoc test after one-way ANOVA (in B1, F = 5.238 p = 0.0072; in B2, F = 5.806 p = 0.0043; in B3, F = 4.217 p = 0.0179; in C1, F = 6.151 p = 0.0032; in C2, F = 9.399 p = 0.0002; in C3, F = 2.826 p = 0.0648).

in CA2 was similar during all 5 trials (Figures 7F and S11), further supporting the conclusion that mean levels of LEC activity do not distinguish a novel from familiar animal.

The above results thus indicate that LEC inputs to CA2, which are critical for social memory, are significantly activated during social interactions with both novel and familiar mice, and this mean level of activation is greater for social than non-social interactions. We next examined whether the MEC inputs to CA2, which are not necessary for social memory, are also activated by social exploration, and how this compares to MEC activity during non-social exploration. Similar to our LEC recordings, we expressed GCaMP7f in MEC and performed fiber photometry recordings from CA2. In contrast to our findings with LEC inputs, we found that MEC inputs to CA2 showed only weak, non-significant changes in Ca^{2+} signals during interactions with a novel or familiar mouse (Figure S12), consistent with our behavioral findings on the lack of role of MEC in social memory. We observed variable responses of MEC to objects.

DISCUSSION

Although the medial and lateral divisions of EC are well known to provide, respectively, distinct spatial and non-spatial forms of information to the hippocampus (Connor and Knierim, 2017; Reagh and Yassa, 2014), there has been no systematic study of the relative roles of these cortical subdivisions and their routes of information flow in hippocampal-dependent social memory. Furthermore, although there have been several proposed models for the function of convergent direct and indirect cortical inputs to CA1, CA2, and CA3 regions, including the detection of novelty (Lisman and Grace, 2005) or salience (Dudman et al., 2007), memory specificity (Basu et al., 2016), or prevention of memory interference (Kaifosh and Losonczy, 2016), there have been relatively few experimental tests of such proposals. Here, we provide the first direct evidence that the direct inputs from LEC to CA2 are critical for both the encoding and recall of social memory. Moreover, our data suggest that the mean level of LEC activity may not provide a robust social novelty signal to CA2,

Please cite this article in press as: Lopez-Rojas et al., A direct lateral entorhinal cortex to hippocampal CA2 circuit conveys social information required for social memory, Neuron (2022), https://doi.org/10.1016/j.neuron.2022.01.028

CellPress
OPEN ACCESS

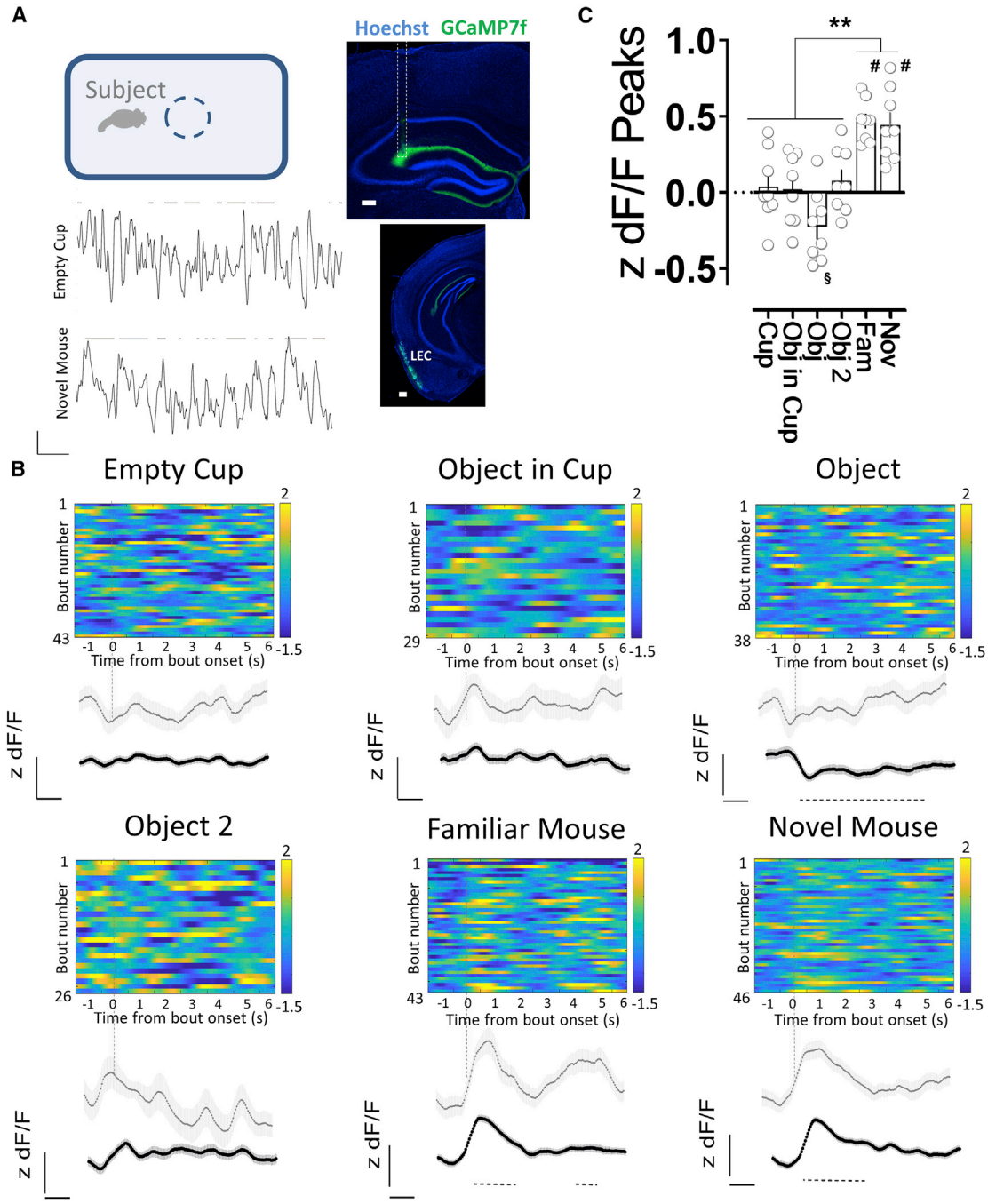

Figure 6. Activity of direct lateral entorhinal cortex input to dorsal CA2 increases during social exploration

(A) Fiber photometry recordings of GCaMP7f fluorescence in lateral entorhinal cortex (LEC) inputs to CA2 in dorsal hippocampus while an animal explores different items in an open arena. Coronal section of the hippocampus showing the expression of GCaMP7f and the optical fiber location (dashed outline) in mice previously injected with AAV in LEC. The lower panel of the inset shows a coronal section of the infected LEC area. GCaMP7f *Z*-scored dF/F traces during bouts of interaction (lines at top) with a novel object (empty cup) or a novel mouse. Scale bars: inset 200 μm and traces 1 z unit dF/F, 10 s.

(B) Exploration of a littermate or a novel conspecific, but not novel objects, is associated with an increase in GCaMP7f fluorescence intensity in LEC inputs in dorsal CA2. Color-coded *Z*-scored dF/F traces from a single animal aligned to the time of interaction. Gray trace shows average fluorescence from all interaction bouts of a given type for that animal. Black traces show average of all animals (n = 8). Dashed line below the traces indicates the time window with a significant difference with respect to baseline (based on the 95th percentile of the bootstrapped confidence interval [Jean-Richard-dit-Bressel et al., 2020]). Scale bars: 0.5 z units dF/F, 1 s. Color scale, numbers indicate range of Z scores.

(C) Mean peak fluorescence values for given bouts of exploration averaged from all animals.

§$p < 0.05$, #$p < 0.0001$ one-sample t test against "0." **$p < 0.01$, Holm-Sidak's post hoc test after repeated measures one-way ANOVA ($F = 19.53$ $p < 0.0001$).

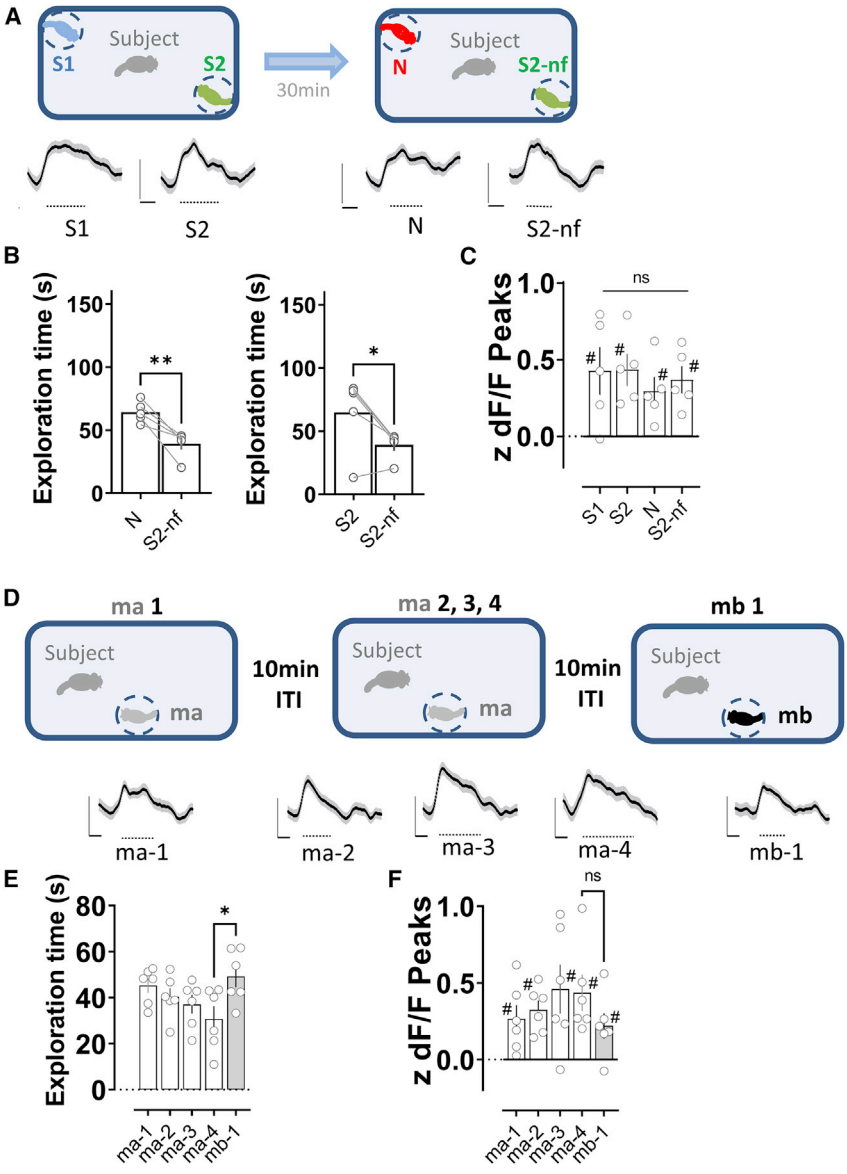

Figure 7. Activity of direct lateral entorhinal cortex input to dorsal CA2 during repeated social exploration of a novel stimulus conspecific

(A) Two-choice social memory task used above. In the learning trial, subject mice explored the arena containing two novel stimulus mice (S1 and S2) for 5 min. The subject mouse was then removed from the arena for a 30 min inter-trial interval. In the recall trial, the subject mouse was reintroduced to the arena and allowed to explore two stimulus mice for another 5 min. One stimulus mouse was previously encountered in the learning trial (S2, which is now familiar, S2-nf) while the other stimulus mouse from the learning trial (S1) was replaced by a third novel mouse (N). Mouse replaced (S1 or S2) was chosen at random. Bottom traces show *Z*-scored dF/F average traces from all subject animals (n = 5), aligned to the time of interaction. Dashed line below the traces indicates the time window with a significant difference with respect to baseline (based on the 95th percentile of the bootstrapped confidence interval; Jean-Richard-dit-Bressel et al., 2020).

(B) Left, social memory is manifest by the preferential exploration of the novel mouse (N) in recall trial compared with now-familiar mouse S2-nf. Right, social memory is also manifest by decreased exploration of S2-nf in recall compared with learning trials.

(C) Mean LEC peak Ca^{2+} signals during bouts of exploration of indicated stimulus mice in learning (S1 and S2) and recall (S2-nf and N) trials. Although we saw significant increases in LEC Ca^{2+} levels in each of the four conditions relative to baseline, the signals did not differ among the four conditions (repeated measures one-way ANOVA, F = 0.3135 p = 0.8154). Each symbol is from a different mouse. *p < 0.05, **p < 0.01 t test; #p < 0.05 one-sample t test against "0."

(D) Five-trial social memory assay. Bottom traces show *Z*-scored dF/F average traces from all subject animals (n = 6), aligned to the time of interaction. Dashed line below the traces indicates the time window with a significant difference with respect to baseline (as described above).

(E) A subject mouse habituated to repeated presentations of the same mouse (ma, trials 1–4: ma-1, ma-2, ma-3 and ma-4) and dishabituated to a novel mouse (mb, trial 5: mb-1), as evidenced by changes in exploration times in a trial.

(F) Despite the increase in familiarity, the level of activity of LEC terminals in dorsal CA2 did not significantly decrease during trials 1–4. Moreover, the introduction of the second novel mouse in trial 5 did not result in a higher level of LEC activity. *p < 0.05 Holm-Sidak's post hoc test after repeated measures one-way ANOVA (F = 3.746 p = 0.0197). #p < 0.05 one-sample t test against "0."

implying that social novelty detection may depend on a local computation in CA2.

Compared with our detailed understanding of how MEC encodes spatial information through grid cell, border cell, and head-direction cell activity (Moser et al., 2017; Rowland et al., 2016), we know much less about how representations encoded in the LEC contribute to hippocampal-dependent memory. Recent work in animal models and humans suggests that LEC might process temporal memories (Montchal et al., 2019; Tsao et al., 2018), egocentric information (Wang et al., 2018), and episodic-like representations (Vandrey et al., 2020). Also, input from LEC to the hippocampus has been found to be required for olfactory associational learning (Li et al., 2017). This emerging picture points to more varied and higher-order representations in LEC than the more selective spatial information conveyed by MEC. Indeed, LEC constitutes a central cortical hub, forming one of the richest sets of association connections of any brain region (Bota et al., 2015; Swanson and Kohler, 1986). Our current results extend these findings by showing that the encoding and recall of social memory require the direct input of multisensory information from LEC, but not MEC, to the dorsal CA2 region of the hippocampus.

Using a combination of *ex vivo* electrophysiology, optogenetic and chemogenetic behavioral studies, and fiber

photometry, we explored the relative roles of the direct LEC and MEC inputs in the synaptic excitation of CA2 PNs, social memory behavior, and the encoding of social exploration. At the physiological level, we found that LEC provides a significantly stronger direct excitatory drive to CA2 PNs compared with MEC. The preferential excitation of CA2 by LEC compared with MEC was reflected in our behavioral results showing that LEC but not MEC inputs to dorsal CA2 were required for CA2-dependent social memory. The selective behavioral role of LEC compared with MEC in social memory is consistent with our findings that LEC was more strongly and selectively activated by social exploration compared with MEC, as revealed by c-Fos labeling and fiber photometry experiments. However, as it has been reported that not all CA2 PNs have dendrites that arborize into the SLM (Helton et al., 2019), there might be an heterogeneous response of CA2 PNs to EC activation.

In addition to defining the relative importance of LEC and MEC in social memory, our study also provides evidence that the direct LEC inputs to CA2 are more critical for social memory compared with the indirect EC inputs that arrive in CA2 either through a trisynaptic path (EC → DG → CA3 → CA2) or a disynaptic path (EC → DG → CA2). Although a prior study suggested that the EC inputs to DG were also important for social memory (Leung et al., 2018), the experimental approaches used make it difficult to distinguish whether the effects of the EC inputs were, in fact, mediated through their synaptic connections with DG rather than with another target, including CA2. Our finding that direct silencing of dorsal DG fails to suppress social memory is consistent with the view that the EC inputs participate in social memory predominantly through their direct excitation of CA2. Although our study cannot definitively rule out the possibility that the direct EC inputs to CA3 may also participate in social memory, the EC inputs provide only weak excitation of CA3 compared with CA2 (Sun et al., 2017). Moreover, it was previously reported that silencing through a chemogenetic approach dorsal CA3, and to some extent dorsal DG, caused no significant impairment in social memory (Chiang et al., 2018).

In addition to the classic division of hippocampus along its transverse axis into DG, CA3, CA2, and CA1 regions, there is a well-known heterogeneity in anatomical connectivity, function, and behavior along the longitudinal (dorsal-ventral or septal-temporal) axis of the hippocampus (Strange et al., 2014). We have focused on the projections of EC to the dorsal region of CA2, as dorsal CA2 is critical for social memory (Hitti and Siegelbaum, 2014; Meira et al., 2018). In contrast, it is the ventral portions of both CA1 (Okuyama et al., 2016) and CA3 (Chiang et al., 2018) that are important for social memory, with neither dorsal CA1 (Okuyama et al., 2016) nor dorsal CA3 (Chiang et al., 2018) playing significant roles. The apparent dichotomy between the importance of dorsal CA2 versus ventral CA1/CA3 was resolved by Meira et al. (2018), who found that dorsal CA2 participates in social memory through its longitudinal projections to the ventral hippocampus. The extent to which ventral CA2 participates in social memory and the importance of the direct entorhinal inputs to ventral CA2 remain to be determined. Other questions that remain to be explored include whether LEC also influences CA2 place fields or their global remapping in response to social stimuli (Alexander et al., 2016) or how LEC activity might impact longer-term social recognition memory.

Our study also provides insight into the nature of the computations that might be performed by the convergence of direct and indirect cortico-hippocampal pathways onto a common pyramidal cell target. As noted above, one interesting model posits that this circuitry is important for the ability of the hippocampus to serve as a novelty detector (Lisman and Grace, 2005), with the direct inputs providing an immediate representation of sensory experience that is then compared with mnemonic information from stored representations in DG and CA3 conveyed by the indirect inputs to either CA1 or CA2. In this manner, the hippocampus may gauge both familiarity, the ability to distinguish a novel from a previously encountered stimulus, and enable detailed recollection of the rich sensory information that a given episodic memory comprises (Hasselmo and Wyble, 1997).

In vivo recordings have previously shown that a significant subset of CA2 PNs fire preferentially during interactions with a novel animal compared with a familiar littermate (Donegan et al., 2020; Leroy et al., 2018). Moreover, CA2 population firing rates can be used to train a linear decoder to distinguish whether an animal is interacting with a novel or familiar animal, indicating that CA2 encodes social novelty (Donegan et al., 2020). Our finding that the global activity conveyed by LEC to CA2, assessed by mean population Ca^{2+} levels measured through fiber photometry, was similar during exploration of novel and familiar animals suggests that the LEC itself may not be the primary source of the social novelty signal. This, in turn, implies that the determination of social novelty may be computed locally in CA2. One important caveat is that these conclusions are based on measures of mean LEC input activity to CA2 and do not rule out the presence of two or more distinct subpopulations of LEC neurons whose activity is selectively increased or decreased by social novelty, which could provide CA2 with significant information on social novelty with little mean change in overall LEC activity.

One potential source of novelty information to CA2 is through the inputs it receives from the hypothalamic supramammillary nucleus, which has been recently shown to convey social novelty signals to CA2 (Chen et al., 2020). However, it has not yet been shown whether the supramammillary inputs differentiate between a novel versus a familiar animal. Moreover, because the supramammillary inputs preferentially excite inhibitory neurons in the CA2 region (Chen et al., 2020; Robert et al., 2020), it is unclear how such an input could enhance CA2 PN firing to social novelty. Finally, as the computation of novelty requires processing of complex sensory information and its comparison with stored representations, such computations are more likely to be performed in higher-order brain regions.

Here, we propose a model for the computation of social novelty based on the intrinsic circuitry of the hippocampus and the finding that information relayed to CA2 from DG and CA3 through the trisynaptic path elicits strong net feedforward inhibition of CA2 PNs (Chevaleyre and Siegelbaum, 2010). According to this view, the specific set of sensory cues that constitute the unique identity of a given novel or familiar conspecific

would produce a strong activation of CA2 PNs due to the strong excitation they receive from the direct LEC inputs. However, for interactions with a familiar conspecific, activation of the stored representations of that conspecific in DG and/or CA3 would produce feedforward inhibition of CA2, resulting in an enhanced response to a novel social stimulus. Although this possibility seems at odds with our finding that silencing dorsal DG fails to affect social memory or with a study showing that silencing dorsal CA3 also does not alter social memory (Chiang et al., 2018), it is possible that longitudinal projections to CA2 from more ventral regions of hippocampus that are known to participate in social memory may provide the relevant mnemonic information.

As social interactions are at the core of everyday experience, and socially related psychiatric disorders are a serious mental health problem, understanding the interplay of brain structures supporting adaptive social behavior is of key importance. Indeed, the *Df(16)A*$^{+/-}$ mouse line, a genetic model of the human 22q11.2 microdeletion, which is one of the greatest known genetic risk factors for schizophrenia (Karayiorgou et al., 2010), has impaired social memory (Piskorowski et al., 2016) that is associated with impaired CA2 firing responses to social cues and social novelty (Donegan et al., 2020). Interestingly, these mice also have a decrease in CA2 feedforward inhibition due to the loss of parvalbumin-positive interneurons (Piskorowski et al., 2016), whose loss is also seen in the general population of individuals with schizophrenia and bipolar disorder (Benes et al., 1998; Knable et al., 2004). According to our above model, such a decrease in feedforward inhibition due to trisynaptic inputs could contribute to the impaired social novelty detection. The idea that alterations in the CA2 cortical-hippocampal circuit may contribute to abnormal social behaviors is further suggested by the finding of EC dysfunction in schizophrenic patients (Baiano et al., 2008; Krimer et al., 1997; Schultz et al., 2010). Furthermore, neurons in LEC superficial layers are particularly susceptible to damage in early Alzheimer's disease stages (Gómez-Isla et al., 1996; Khan et al., 2014; Kobro-Flatmoen et al., 2016), which could also contribute to abnormal social memory associated with this disorder. Thus, elucidating fundamental questions concerning the role of LEC in physiological conditions might provide insights into better preventive and palliative treatments in pathological neuropsychiatric and neurodegenerative contexts.

STAR★METHODS

Detailed methods are provided in the online version of this paper and include the following:

SUPPLEMENTAL INFORMATION

Supplemental information can be found online at https://doi.org/10.1016/j.neuron.2022.01.028.

ACKNOWLEDGMENTS

We thank members of the Siegelbaum laboratory for comments and discussions on the manuscript, L.M. Boyle for pilot calcium imaging experiments, and H.S. Chen for helping with immunostaining. This work was supported by R01-MH104602 and R01-MH106629 from NIH to S.A.S.

AUTHOR CONTRIBUTIONS

J.L.-R. and S.A.S. conceptualized the research; J.L.-R. carried out experiments and analyzed data; C.A.S. carried out fiber photometry experiments. F.L. carried out rabies tracing experiments; J.L.-R. wrote the original draft of the manuscript; J.L.-R. and S.A.S. reviewed and edited the manuscript with input from all authors; S.A.S. and E.R.K. supervised the research and acquired funding.

DECLARATION OF INTERESTS

The authors declare no competing interests.

Received: August 2, 2021
Revised: December 21, 2021
Accepted: January 24, 2022
Published: February 17, 2022

REFERENCES

Alexander, G.M., Farris, S., Pirone, J.R., Zheng, C., Colgin, L.L., and Dudek, S.M. (2016). Social and novel contexts modify hippocampal CA2 representations of space. Nat. Commun. *7*, 10300.

Arbuckle, E.P., Smith, G.D., Gomez, M.C., and Lugo, J.N. (2015). Testing for odor discrimination and habituation in mice. J. Vis. Exp. e52615, 10.3791/52615.

Baiano, M., Perlini, C., Rambaldelli, G., Cerini, R., Dusi, N., Bellani, M., Spezzapria, G., Versace, A., Balestrieri, M., Mucelli, R.P., et al. (2008). Decreased entorhinal cortex volumes in schizophrenia. Schizophr. Res. *102*, 171–180.

Basu, J., Zaremba, J.D., Cheung, S.K., Hitti, F.L., Zemelman, B.V., Losonczy, A., and Siegelbaum, S.A. (2016). Gating of hippocampal activity, plasticity, and memory by entorhinal cortex long-range inhibition. Science *351*, aaa5694.

Benes, F.M., Kwok, E.W., Vincent, S.L., and Todtenkopf, M.S. (1998). A reduction of nonpyramidal cells in sector CA2 of schizophrenics and manic depressives. Biol. Psychiatry *44*, 88–97.

Bota, M., Sporns, O., and Swanson, L.W. (2015). Architecture of the cerebral cortical association connectome underlying cognition. Proc. Natl. Acad. Sci. USA *112*, E2093–E2101.

Chen, S., He, L., Huang, A.J.Y., Boehringer, R., Robert, V., Wintzer, M.E., Polygalov, D., Weitemier, A.Z., Tao, Y., Gu, M., et al. (2020). A hypothalamic novelty signal modulates hippocampal memory. Nature *586*, 270–274.

Chevaleyre, V., and Siegelbaum, S.A. (2010). Strong CA2 pyramidal neuron synapses define a powerful disynaptic cortico-hippocampal loop. Neuron *66*, 560–572.

Chiang, M.-C., Huang, A.J.Y., Wintzer, M.E., Ohshima, T., and McHugh, T.J. (2018). A role for CA3 in social recognition memory. Behav. Brain Res. *354*, 22–30.

Connor, C.E., and Knierim, J.J. (2017). Integration of objects and space in perception and memory. Nat. Neurosci. *20*, 1493–1503.

Donegan, M.L., Stefanini, F., Meira, T., Gordon, J.A., Fusi, S., and Siegelbaum, S.A. (2020). Coding of social novelty in the hippocampal CA2 region and its disruption and rescue in a 22q11.2 microdeletion mouse model. Nat. Neurosci. *23*, 1365–1375.

Dudman, J.T., Tsay, D., and Siegelbaum, S.A. (2007). A role for synaptic inputs at distal dendrites: instructive signals for hippocampal long-term plasticity. Neuron *56*, 866–879.

Eichenbaum, H., Yonelinas, A.P., and Ranganath, C. (2007). The medial temporal lobe and recognition memory. Annu. Rev. Neurosci. *30*, 123–152.

Fernández, G., and Morris, R.G.M. (2018). Memory, novelty and prior knowledge. Trends Neurosci. *41*, 654–659.

Fujimaru, Y., and Kosaka, T. (1996). The distribution of two calcium binding proteins, calbindin D-28K and parvalbumin, in the entorhinal cortex of the adult mouse. Neurosci. Res. *24*, 329–343.

Gómez-Isla, T., Price, J.L., McKeel, D.W., Morris, J.C., Growdon, J.H., and Hyman, B.T. (1996). Profound loss of layer II entorhinal cortex neurons occurs in very mild Alzheimer's disease. J. Neurosci. *16*, 4491–4500.

Hasselmo, M.E., and Wyble, B.P. (1997). Free recall and recognition in a network model of the hippocampus: simulating effects of scopolamine on human memory function. Behav. Brain Res. *89*, 1–34.

Helton, T.D., Zhao, M., Farris, S., and Dudek, S.M. (2019). Diversity of dendritic morphology and entorhinal cortex synaptic effectiveness in mouse CA2 pyramidal neurons. Hippocampus *29*, 78–92.

Hitti, F.L., and Siegelbaum, S.A. (2014). The hippocampal CA2 region is essential for social memory. Nature *508*, 88–92.

Jean-Richard-dit-Bressel, P., Clifford, C.W.G., and McNally, G.P. (2020). Analyzing event-related transients: confidence intervals, permutation tests, and consecutive thresholds. Front. Mol. Neurosci. *13*, 14.

Kafkas, A., and Montaldi, D. (2018). How do memory systems detect and respond to novelty? Neurosci. Lett. *680*, 60–68.

Kaifosh, P., and Losonczy, A. (2016). Mnemonic functions for nonlinear dendritic integration in hippocampal pyramidal circuits. Neuron *90*, 622–634.

Karayiorgou, M., Simon, T.J., and Gogos, J.A. (2010). 22q11.2 microdeletions: linking DNA structural variation to brain dysfunction and schizophrenia. Nat. Rev. Neurosci. *11*, 402–416.

Karlsson, S.A., Haziri, K., Hansson, E., Kettunen, P., and Westberg, L. (2015). Effects of sex and gonadectomy on social investigation and social recognition in mice. BMC Neurosci. *16*, 83.

Khan, U.A., Liu, L., Provenzano, F.A., Berman, D.E., Profaci, C.P., Sloan, R., Mayeux, R., Duff, K.E., and Small, S.A. (2014). Molecular drivers and cortical spread of lateral entorhinal cortex dysfunction in preclinical Alzheimer's disease. Nat. Neurosci. *17*, 304–311.

Knable, M.B., Barci, B.M., Webster, M.J., Meador-Woodruff, J., Torrey, E.F., and Stanley, Neuropathology Consortium. (2004). Molecular abnormalities of the hippocampus in severe psychiatric illness: postmortem findings from the Stanley Neuropathology Consortium. Mol. Psychiatry *9*, 609–620.

Kobro-Flatmoen, A., Nagelhus, A., and Witter, M.P. (2016). Reelin-immunoreactive neurons in entorhinal cortex layer II selectively express intracellular amyloid in early Alzheimer's disease. Neurobiol. Dis. *93*, 172–183.

Kogan, J.H., Frankland, P.W., and Silva, A.J. (2000). Long-term memory underlying hippocampus-dependent social recognition in mice. Hippocampus *10*, 47–56.

Kohara, K., Pignatelli, M., Rivest, A.J., Jung, H.-Y., Kitamura, T., Suh, J., Frank, D., Kajikawa, K., Mise, N., Obata, Y., et al. (2014). Cell type–specific genetic and optogenetic tools reveal hippocampal CA2 circuits. Nat. Neurosci. *17*, 269–279.

Krimer, L.S., Herman, M.M., Saunders, R.C., Boyd, J.C., Hyde, T.M., Carter, J.M., Kleinman, J.E., and Weinberger, D.R. (1997). A qualitative and quantitative analysis of the entorhinal cortex in schizophrenia. Cereb. Cortex *7*, 732–739.

Krueger-Burg, D., Winkler, D., Mitkovski, M., Daher, F., Ronnenberg, A., Schlüter, O.M., Dere, E., and Ehrenreich, H. (2016). The SocioBox: a novel paradigm to assess complex social recognition in male mice. Front. Behav. Neurosci. *10*, 151.

Leitner, F.C., Melzer, S., Lütcke, H., Pinna, R., Seeburg, P.H., Helmchen, F., and Monyer, H. (2016). Spatially segregated feedforward and feedback neurons support differential odor processing in the lateral entorhinal cortex. Nat. Neurosci. *19*, 935–944.

Leroy, F., Brann, D.H., Meira, T., and Siegelbaum, S.A. (2017). Input-timing-dependent plasticity in the hippocampal CA2 region and its potential role in social memory. Neuron *95*, 1089–1102.e5.

Leroy, F., Park, J., Asok, A., Brann, D.H., Meira, T., Boyle, L.M., Buss, E.W., Kandel, E.R., and Siegelbaum, S.A. (2018). A circuit from hippocampal CA2 to lateral septum disinhibits social aggression. Nature *564*, 213–218.

Leung, C., Cao, F., Nguyen, R., Joshi, K., Aqrabawi, A.J., Xia, S., Cortez, M.A., Snead, O.C., Kim, J.C., and Jia, Z. (2018). Activation of entorhinal cortical projections to the dentate gyrus underlies social memory retrieval. Cell Rep. *23*, 2379–2391.

Li, Y., Xu, J., Liu, Y., Zhu, J., Liu, N., Zeng, W., Huang, N., Rasch, M.J., Jiang, H., Gu, X., et al. (2017). A distinct entorhinal cortex to hippocampal CA1 direct circuit for olfactory associative learning. Nat. Neurosci. *20*, 559–570.

Lisman, J.E., and Grace, A.A. (2005). The hippocampal-VTA loop: controlling the entry of information into long-term memory. Neuron *46*, 703–713.

Lopes, G., Bonacchi, N., Frazão, J., Neto, J.P., Atallah, B.V., Soares, S., Moreira, L., Matias, S., Itskov, P.M., Correia, P.A., et al. (2015). Bonsai: an event-based framework for processing and controlling data streams. Front. Neuroinform. *9*, 7.

Martianova, E., Aronson, S., and Proulx, C.D. (2019). Multi-fiber photometry to record neural activity in freely-moving animals. J. Vis. Exp. e60278, 10.3791/60278.

McHugh, T.J., Jones, M.W., Quinn, J.J., Balthasar, N., Coppari, R., Elmquist, J.K., Lowell, B.B., Fanselow, M.S., Wilson, M.A., and Tonegawa, S. (2007). Dentate gyrus NMDA receptors mediate rapid pattern separation in the hippocampal network. Science *317*, 94–99.

Meira, T., Leroy, F., Buss, E.W., Oliva, A., Park, J., and Siegelbaum, S.A. (2018). A hippocampal circuit linking dorsal CA2 to ventral CA1 critical for social memory dynamics. Nat. Commun. *9*, 4163.

Middleton, S.J., and McHugh, T.J. (2020). CA2: a highly connected intrahippocampal relay. Annu. Rev. Neurosci. *43*, 55–72.

Montchal, M.E., Reagh, Z.M., and Yassa, M.A. (2019). Precise temporal memories are supported by the lateral entorhinal cortex in humans. Nat. Neurosci. *22*, 284–288.

Moser, E.I., Moser, M.-B., and McNaughton, B.L. (2017). Spatial representation in the hippocampal formation: a history. Nat. Neurosci. *20*, 1448–1464.

Moser, E.I., Roudi, Y., Witter, M.P., Kentros, C., Bonhoeffer, T., and Moser, M.-B. (2014). Grid cells and cortical representation. Nat. Rev. Neurosci. *15*, 466–481.

Okuyama, T., Kitamura, T., Roy, D.S., Itohara, S., and Tonegawa, S. (2016). Ventral CA1 neurons store social memory. Science *353*, 1536–1541.

Oliva, A., Fernández-Ruiz, A., Leroy, F., and Siegelbaum, S.A. (2020). Hippocampal CA2 sharp-wave ripples reactivate and promote social memory. Nature *587*, 264–269.

Piskorowski, R.A., Nasrallah, K., Diamantopoulou, A., Mukai, J., Hassan, S.I., Siegelbaum, S.A., Gogos, J.A., and Chevaleyre, V. (2016). Age-dependent specific changes in area CA2 of the hippocampus and social memory deficit in a mouse model of the 22q11.2 deletion syndrome. Neuron *89*, 163–176.

Reagh, Z.M., and Yassa, M.A. (2014). Object and spatial mnemonic interference differentially engage lateral and medial entorhinal cortex in humans. Proc. Natl. Acad. Sci. USA *111*, E4264–E4273.

Robert, V., Therreau, L., Huang, A.J.Y., Boehringer, R., Polygalov, D., McHugh, T., Chevaleyre, V., and Piskorowski, R.A. (2020). Local circuit allowing hypothalamic control of hippocampal area CA2 activity and consequences for CA1. eLife *10*, e63352.

Rowland, D.C., Roudi, Y., Moser, M.-B., and Moser, E.I. (2016). Ten years of grid cells. Annu. Rev. Neurosci. *39*, 19–40.

Schultz, C.C., Koch, K., Wagner, G., Roebel, M., Schachtzabel, C., Nenadic, I., Albrecht, C., Reichenbach, J.R., Sauer, H., and Schlösser, R.G.M. (2010). Psychopathological correlates of the entorhinal cortical shape in schizophrenia. Eur. Arch. Psychiatry Clin. Neurosci. *260*, 351–358.

Srinivas, K.V., Buss, E.W., Sun, Q., Santoro, B., Takahashi, H., Nicholson, D.A., and Siegelbaum, S.A. (2017). The dendrites of CA2 and CA1 pyramidal neurons differentially regulate information flow in the cortico-hippocampal circuit. J. Neurosci. *37*, 3276–3293.

Steward, O. (1976). Topographic organization of the projections from the entorhinal area to the hippocampal formation of the rat. J. Comp. Neurol. *167*, 285–314.

Strange, B.A., Witter, M.P., Lein, E.S., and Moser, E.I. (2014). Functional organization of the hippocampal longitudinal axis. Nat. Rev. Neurosci. *15*, 655–669.

Sun, Q., Sotayo, A., Cazzulino, A.S., Snyder, A.M., Denny, C.A., and Siegelbaum, S.A. (2017). Proximodistal heterogeneity of hippocampal CA3 pyramidal neuron intrinsic properties, connectivity, and reactivation during memory recall. Neuron *95*, 656–672.e3.

Sun, Q., Srinivas, K.V., Sotayo, A., and Siegelbaum, S.A. (2014). Dendritic Na+ spikes enable cortical input to drive action potential output from hippocampal CA2 pyramidal neurons. eLife *3*, e04551.

Swanson, L.W., and Köhler, C. (1986). Anatomical evidence for direct projections from the entorhinal area to the entire cortical mantle in the rat. J. Neurosci. *6*, 3010–3023.

Tsao, A., Sugar, J., Lu, L., Wang, C., Knierim, J.J., Moser, M.-B., and Moser, E.I. (2018). Integrating time from experience in the lateral entorhinal cortex. Nature *561*, 57–62.

Vandrey, B., Garden, D.L.F., Ambrozova, V., McClure, C., Nolan, M.F., and Ainge, J.A. (2020). Fan cells in layer 2 of the lateral entorhinal cortex are critical for episodic-like memory. Curr. Biol. *30*, 169–175.e5.

Wang, C., Chen, X., Lee, H., Deshmukh, S.S., Yoganarasimha, D., Savelli, F., and Knierim, J.J. (2018). Egocentric coding of external items in the lateral entorhinal cortex. Science *362*, 945–949.

Watarai, A., Tao, K., Wang, M.Y., and Okuyama, T. (2021). Distinct functions of ventral CA1 and dorsal CA2 in social memory. Curr. Opin. Neurobiol. *68*, 29–35.

Yang, M., and Crawley, J.N. (2009). Simple behavioral assessment of mouse olfaction. Curr. Protoc. Neurosci. 1–12.

Zhu, H., Aryal, D.K., Olsen, R.H.J., Urban, D.J., Swearingen, A., Forbes, S., Roth, B.L., and Hochgeschwender, U. (2016). Cre-dependent DREADD (Designer Receptors Exclusively Activated by Designer Drugs) mice. Genesis *54*, 439–446.

Please cite this article in press as: Lopez-Rojas et al., A direct lateral entorhinal cortex to hippocampal CA2 circuit conveys social information required for social memory, Neuron (2022), https://doi.org/10.1016/j.neuron.2022.01.028

STAR★METHODS

KEY RESOURCES TABLE

REAGENT or RESOURCE	SOURCE	IDENTIFIER
Antibodies		
anti-c-Fos	Synaptic Systems	Cat# 226 003; RRID:AB_2231974
anti-RGS14	UC Davis/NIH NeuroMab Facility	Cat# 75-170; RRID:AB_2179931
streptavidin conjugated to Alexa 647	ThermoFisher Scientific	Cat# S21374; RRID:AB_2336066
anti-mouse IgG2a conjugated to Alexa 488	ThermoFisher Scientific	Cat# A21131; RRID:AB_2535771
anti-rabbit conjugated to Alexa 647	ThermoFisher Scientific	Cat# A31573; RRID:AB_2536183
Bacterial and virus strains		
AAV2/9 hSyn.hChR2 (H134R).eYFP.WPRE.hGH	UPenn Viral Vector Core	N/A
AAV2/9 CaMKII.ArchT-GFP	UNC Vector Core	N/A
pGP-AAV-syn-jGCaMP7f-WPRE	Dana et al. Nat Methods. 2019 Jul;16(7):649-657. doi:10.1038/s41592-019-0435-6.	Addgene Cat# 104488-AAV8
AAV2/9-CaMKIIa-hM4D(Gi)-mCherry	Roth lab DREADDs (unpublished)	Addgene Cat# 50477-AAV9
AAV2/8 syn.DIO.TVA.2A.GFP.2A.B19G	UNC Vector Core	Addgene Cat# 52473
rabies SAD.B19.EnvA.ΔG.mCherry	Salk institute Vector Core	Addgene Cat# 32636
Experimental models: Organisms/strains		
C57BL/6J mice	The Jackson Laboratory	Cat# 000664
POMC-Cre mice	The Jackson Laboratory	Cat# 010714
R26-hM4Di/mCitrine mice	The Jackson Laboratory	Cat# 026219
Amigo-2 Cre mice	The Jackson Laboratory	Cat# 030215
Software and algorithms		
AnyMaze Version: 7.09	Stoelting Co.	https://www.any-maze.com/
AxoGraph Version: 1.7.0	AxoGraph	https://axograph.com/
Bonsai Version: 2.6.3	Open Ephys	https://open-ephys.org/bonsai
MATLAB Version: R2019b	Mathworks	https://www.mathworks.com/
Photometry_data_processing (Matlab)	Martianova et al., 2019; doi: 10.3791/60278.	https://github.com/katemartian/Photometry_data_processing
Prism Version: 9.3.0	GraphPad Software	https://www.graphpad.com/scientific-software/prism/
ZEN Version: Black 2.3	Zeiss	https://www.zeiss.com/microscopy/int/products/microscope-software/zen.html

RESOURCE AVAILABILITY

Lead contact

Further information and requests for resources and reagents should be directed to and will be fulfilled by the Lead Contact, Jeffrey Lopez-Rojas (jl5545@columbia.edu).

Materials availability

This study did not generate unique reagents.

Data and code availability

Data reported in this paper will be shared by the lead contact upon request.

This paper does not report original code.

Any additional information required to reanalyze the data reported in this work paper is available from the Lead Contact upon request.

EXPERIMENTAL MODEL AND SUBJECT DETAILS

All animal procedures were performed in accordance with the regulations of the Columbia University IACUC. 8- to 12-week-old male mice were used for most experiments. Male mice were used exclusively in this study, as there are significant differences in sociability and social recognition between male and female mice (Karlsson et al., 2015; Krueger-Burg et al., 2016) that would complicate the present analyses. Future work will be required to study entorhinal cortical contributions to social cognition in females. The mice were group housed and maintained in a temperature- and humidity-controlled room on a 12:12 h light/dark cycle. All animals were provided with food and water ad libitum. All tests were conducted during the light cycle. Experiments were scored by an individual blind to the genotype and experimental design.

Wild-type C57BL/6J male mice (JAX Stock No: 000664) were obtained from the Jackson Laboratory. POMC-Cre(+/-) male mice (JAX Stock No: 010714) were obtained from Jackson Laboratory and were bred with R26-hM4Di/mCitrine female homozygous (JAX Stock No: 026219). Amigo-2 Cre male mice were obtained from Jackson Laboratory (JAX Stock No: 030215).

METHOD DETAILS

Viral injections

Viral injections were performed as described previously (Leroy et al., 2017, 2018). Briefly, mice were anesthetized with isoflurane and placed in a stereotaxic apparatus. A craniotomy was performed above the target region and a glass micropipette was used for viral injection. Injections were performed using a nano-inject II (Drummond Scientific). Twenty-three nl of solution were delivered every 15 s until the total amount was reached. The micropipette was retracted after 5 min. We bilaterally injected 368 nl of AAV2/9 hSyn.hChR2(H134R).eYFP.WPRE.hGH (UPenn Vector Core, titer $3.6*10^{12}$ genome copy (GC) ml^{-1}) or AAV2/9 CaMKII.ArchT-GFP (UNC Vector Core, viral titer $2.2*10^{12}$ GC ml^{-1}) or pGP-AAV-syn-jGCaMP7f-WPRE (Addgene, titer $3.6*10^{12}$ GC ml^{-1}) or AAV2/9-CaMKIIa-hM4D(Gi)-mCherry (Addgene, titer $2.5*10^{12}$ GC ml^{-1}) to the LEC or MEC. The positions were: -3.4 mm AP, +/- 4.7 mm ML and 2.8 mm DV for LEC injections and -4.9 mm, +/- 3.4 mm ML and 2.8 mm DV for MEC injections. Mice were allowed to recover for 2-3 weeks.

Rabies and AAV helper virus injection in CA2

We delivered 50 nl of a G-deleted rabies helper virus AAV2/8 syn.DIO.TVA.2A.GFP.2A.B19G (UNC Vector Core) into the dorsal hippocampus of Amigo2-Cre mouse at the following coordinates AP -1.8 mm, ML +2.5 mm, DV -1.7 mm. Following 2 weeks of recovery and AAV expression, a second surgery was performed and 300 nl of rabies SAD.B19.EnvA.ΔG.mCherry (SAD-B19 strain, Addgene Cat# 32636 prepared by the Salk institute Vector Core) was injected at the same coordinates. Mice were killed 7 d later and the brains cut horizontally between 3.28 and 4.72 mm from Bregma along the dorso–ventral axis for entorhinal cortex imaging or coronally for hippocampus imaging. We randomly selected a series of non-consecutive 60-μm thick brain sections for quantification.

Optical fiber implantation

Multimode fibers of 200 μm core and 0.39 numerical aperture (Thorlabs) were used for behavior experiments. The fibers were glued to a ceramic ferrule and polished to enhance coupling efficiency. The optical fibers were implanted in the dorsal CA2 area (-2.0 mm AP, +/- 2.2 mm ML and 2.0 mm DV) 2 weeks after viral injection and fixed to the skull with dental cement. Fibers were coupled to an external fiber using standard FC connectors via a mating sleeve connected to a 589-nm laser (Laserglow).

Cannula guide implantation

Mice were implanted with a cannula guide extending for 1 mm (Plastics One) below the pedestal. The scalp was removed and holes were drilled (−2.0 mm AP, +/- 1.0 mm ML for DG and −2.0 mm AP, +/- 2.2 mm ML for CA2). Cannula guides were kept in place using super-glue and dental cement. Dummy cannulas (Plastics One) were inserted into the guides. For CNO infusion, mice were placed under light isoflurane anaesthesia and the dummy cannula was removed. The injector cannula protruding 1.5 mm or 0.9 mm from the cannula guide was then inserted for DG or CA2 injections, respectively. One microlitre of a 1 mM CNO solution was infused over 2 min. The injector cannula was removed 2 min after the end of the micro-infusion to avoid pulling out the drug and the dummy cannula was put back. Behavioural testing started 30 min after drug infusion.

Immunohistochemistry

Mice were anesthetized, and brains were processed as previously described (Leroy et al., 2018). Briefly, after fixation in 4% PFA overnight floating sections were prepared and rinsed three times in 1x PBS and then blocked in 1x PBS with 0.5% Triton X-100 and 5% goat serum for 2 hr at room temperature (RT). Incubation with primary antibodies was performed at 4°C overnight in 1 x PBS with 0.5% Triton X-100. Sections were then washed three times in 1x PBS and incubated with secondary antibodies for 2 hr at RT. Hoechst counterstain was applied (Hoechst 33342 at 1:1000 for 30 min in PBS at RT) prior to mounting the slice using fluoromount (Sigma-Aldricht).

For post-hoc immunocytochemistry after patch-clamp recordings, slices were fixed for 1 h in PBS with 4% PFA and Streptavidin conjugated to Alexa 647 (1:500, ThermoFisher Scientific) was applied during secondary incubation following blocking and permeabilization.

For c-Fos labelling, the first incubation was performed with rabbit anti-c-Fos (1:5000, SySy, 226 003) at 4 °C overnight. The secondary incubation was performed with and anti-rabbit conjugated to Alexa 647 (1:500, ThermoFisher A31573).

In vitro electrophysiology

Male mice 7-9 weeks old were anesthetized and killed by decapitation in accordance with institutional regulations, as previously described (Sun et al., 2014, 2017). Hippocampi were dissected out and transverse slices from the dorsal hippocampus were cut with a vibratome (Leica VT1200S, Germany) on in ice-cold dissection solution containing (in mM): 125 NaCl, 2.5 KCl, 20 glucose, 25 $NaHCO_3$, 1.25 NaH_2PO_4, 2 Na-Pyruvate, 2 $CaCl_2$ and 1 $MgCl_2$, equilibrated with 95% O_2/5% CO_2 (pH 7.4). The slices were then incubated at 33°C for 25 min and then kept at room temperature for at least 1 hr before transfer to the recording chamber. All electrophysiological recordings were performed at 31-32°C.

Patch pipettes were pulled from a horizontal micropipette puller (Sutter) and filled with an intracellular solution containing the following (in mM): 135 K-Gluconate, 5 KCl, 0.1 EGTA-Na, 10 HEPES, 2 NaCl, 5 ATP, 0.4 GTP, 10 phosphocreatine and 5 μM biocytin. The pH was adjusted to 7.3 and the osmolarity to 290 mOsm. Pipettes of a 3–5 MΩ tip resistance were used. Whole-cell "blind" patch-clamp configuration was established, and cells were held at −70 to -73 mV. For optogenetics experiments, ChR2 was activated using 470-nm blue light pulses lasting 2 ms; Arch was activated using continuous 590-nm yellow light delivered via a 40x objective placed above the slices through an LED light source (Thorlabs) driven by Axograph software.

Two-choice social memory test

This test was performed as previously described (Oliva et al., 2020). In brief, a subject mouse was habituated for 5 min to a rectangular arena with two empty wire cups in opposite sides. After this, in a learning trial, a novel stimulus male mouse that had no prior contact with the subject mouse was placed inside each of the cups and the subject mouse was allowed to explore the arena with the two novel mice for 5 min. The subject mouse was then isolated for 30 min and one of the stimulus mice was exchanged for a third novel mouse. In the "recall" phase of the test the subject mice were exposed to one of the now-familiar stimulus mice, previously encountered during the learning trial, along with the novel stimulus mouse. Social exploration was quantified as the time spent in active exploration within 5 cm of the perimeter of the cup. We then assessed social memory using a discrimination index:

$$DI = [(\text{time spent exploring mouse N}) - (\text{time spent exploring mouse S})]/$$

$$[(\text{time spent exploring mouse N}) + (\text{time spent exploring mouse S})].$$

For the c-Fos$^+$ EC cell counting experiment, animals were sacrificed 80 min after the task. We randomly selected a series of non-consecutive 60-μm thick horizontal brain sections between 3.28 and 4.72 mm from Bregma along the dorso–ventral axis and stained them for c-Fos and Nissl.

Direct interaction test

This test was adapted from Kogan et al (Kogan et al., 2000). Subject mice were placed in a standard clean cage for a 30 min habituation session immediately prior to the experimental sessions. In trial 1, a novel male juvenile stimulus mouse around 5-weeks-old was then introduced into the cage and activity was monitored for 2 min and scored online for social exploration (sniffing, following and allogrooming) initiated by the test subject. The stimulus mouse was then removed from the cage. In trial 2, after an inter-trail interval of 30 min, the subject mouse was allowed to interact for another 2 min with either the previously encountered stimulus mouse or a novel stimulus mouse. Social memory is normally manifest as the decreased exploration of the same stimulus mouse in trial 2 relative to trial 1. In contrast there is normally no decrease in exploration time when the novel mouse is introduced in trial 2, demonstrating that the decreased exploration of the same mouse in trial 2 is not due to fatigue or loss of motivation over the test duration.

Five-trial social memory test

This test was adapted from previous work (Hitti and Siegelbaum, 2014; Leroy et al., 2018). Subject mice were placed in a standard clean cage for a 30 min habituation session immediately prior to the experimental sessions. Subject mice were presented with a stimulus mouse for four successive 2-min trials, separated by 10 min intertrial interval. On the fifth trial, a second novel stimulus animal was presented.

Buried food test

The mice were food-deprived for 18 h before the test, to improve sensitivity. A pellet of the same chow the animals were regularly fed with was hidden under 1 cm of standard cage bedding. The subject mouse was placed in the cage, and the latency to find the pellet was recorded (Arbuckle et al., 2015; Yang and Crawley, 2009).

Novel object recognition test

A subject mouse was habituated for 5 min to a rectangular arena. After this, two novel objects were placed in opposite sides of the arena and the subject mice were allowed to explore for 10 min (learning phase). After 30 min, one of the objects was

exchanged for another novel one and the subject mice were allowed to explore for 5 min. We then assessed memory using a discrimination index:

$$DI = [(\text{time spent exploring novel object}) - (\text{time spent exploring familiar object})]/ [(\text{time spent exploring novel object}) + (\text{time spent exploring familiar object})].$$

Fiber photometry

A commercially available fiber photometry system, Neurophotometrics FP3002, was used. In brief, recording was accomplished by providing a 415 nm and 470 nm excitation light through the patch-cord for calcium-independent and calcium-dependent fluorescence emission from GCaMP7. Excitation power was adjusted to provide 75 μW of 415 nm and 470 nm light at the tip of the patch cord. Recordings were performed with the bonsai open-source software (Lopes et al., 2015) at 20 Hz. Analysis of the recorded traces was performed as previously described (Jean-Richard-dit-Bressel et al., 2020; Martianova et al., 2019).

QUANTIFICATION AND STATISTICAL ANALYSIS

We used Prism (Graphpad) for statistical analysis. Results presented in the figures are reported as the mean ± s.e.m. The statistical significance was tested by t-tests, paired t-tests or ANOVA (one-way, two-way or repeated measures) followed by Post-hoc Holm-Sidak's multiple comparisons, as indicated. $p<0.05$ was considered significant. "n" refers to the number of cells, slices or animals, as indicated in the figure legends.

Neuron, Volume *110*

Supplemental information

A direct lateral entorhinal cortex to hippocampal CA2 circuit conveys social information required for social memory

Jeffrey Lopez-Rojas, Christopher A. de Solis, Felix Leroy, Eric R. Kandel, and Steven A. Siegelbaum

Title: A direct lateral entorhinal cortex to hippocampal CA2 circuit conveys social information required for social memory

Authors: Jeffrey Lopez-Rojas[a*], Christopher A. de Solis[a], Felix Leroy[a,b], Eric R. Kandel[a,c] and Steven A. Siegelbaum[a*]

[a]Department of Neuroscience, The Kavli Institute for Brain Science, Mortimer B. Zuckerman Mind Brain Behavior Institute, Vagelos College of Physicians and Surgeons, Columbia University, New York, NY, 10027 USA.

[b]Cellular and Systems Neurobiology Research Unit, Instituto de Neurociencias de Alicante, Alicante, Spain.

[c]Howard Hughes Medical Institute, Columbia University, New York, NY, USA

[*]Corresponding authors. E-mail: jl5545@columbia.edu, sas8@columbia.edu

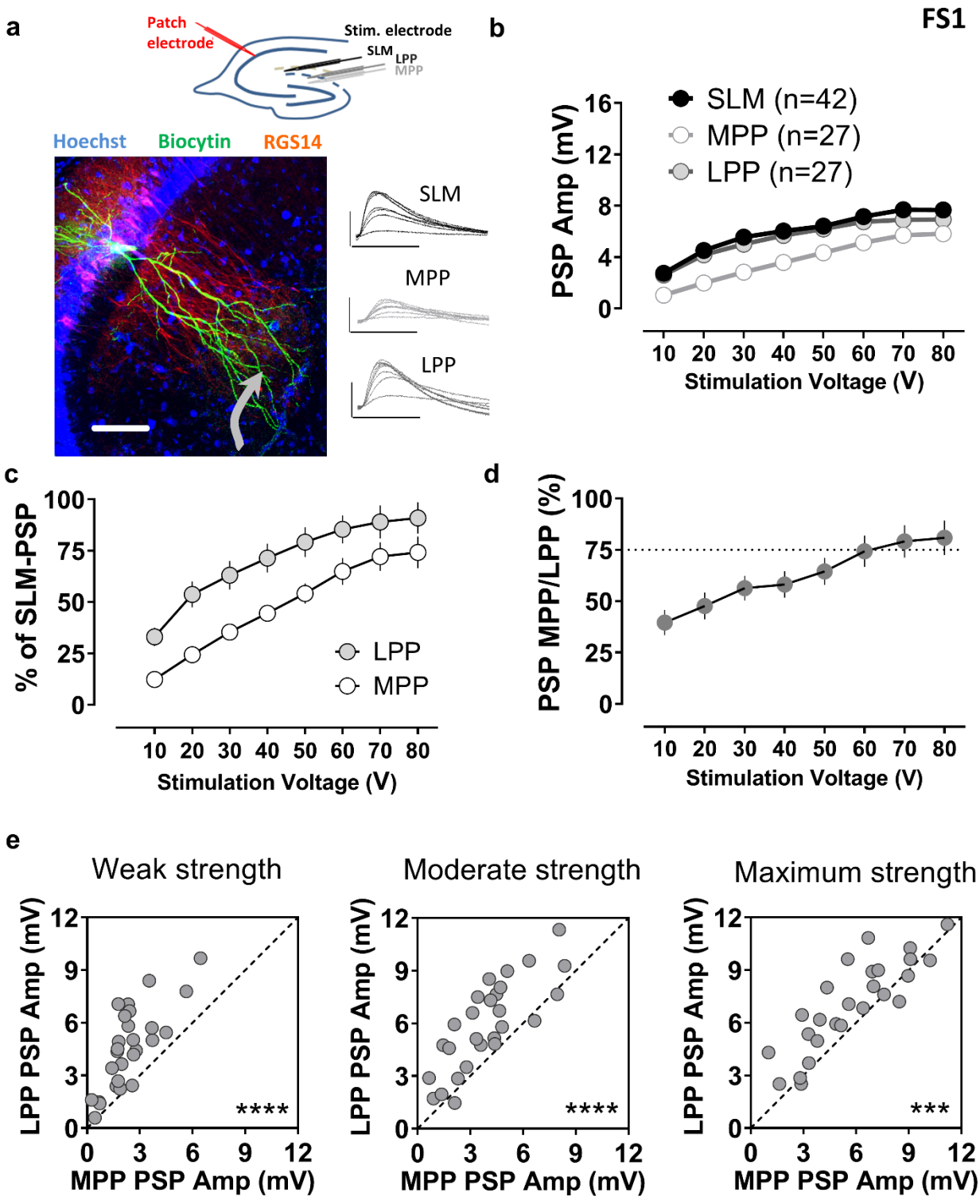

Figure S1. Electrical stimulation of the lateral perforant path evokes a larger intracellular synaptic depolarization of dorsal CA2 pyramidal neurons compared to stimulation of medial perforant path, Related to Figure 1. a, Schematic showing the placement of a stimulating electrode (black) in the stratum lacunosum moleculare (SLM) to

globally activate entorhinal axons or in the outer (LPP) or middle (MPP) molecular layer of the dentate gyrus to selectively stimulate lateral or medial perforant path (LPP or MPP). Synaptic responses were measured using patch clamp recordings from CA2 pyramidal neurons. An image of a patch-clamped biocytin-filled CA2 pyramidal cell and the corresponding voltage responses to stimulation in the indicated regions. **b,** Electrical stimulation at any location evoked a large postsynaptic potential in CA2 pyramidal neurons. The LPP-evoked response (27 cells from 27 slices from 14 animals) was larger than the MPP-evoked response (27 cells from 27 slices from 14 animals), expressed as percentage of the SLM-evoked response (42 cells from 42 slices from 15 animals) (**c**), as a ration of the MPP/LPP response (**d**) or as voltage amplitudes (**e**) over a range of stimulation strengths. Scale bars: **a**: 100 µm and 5 mV/25 ms. ****: $p<0.0001$, ***: $p<0.0001$ paired t-test.

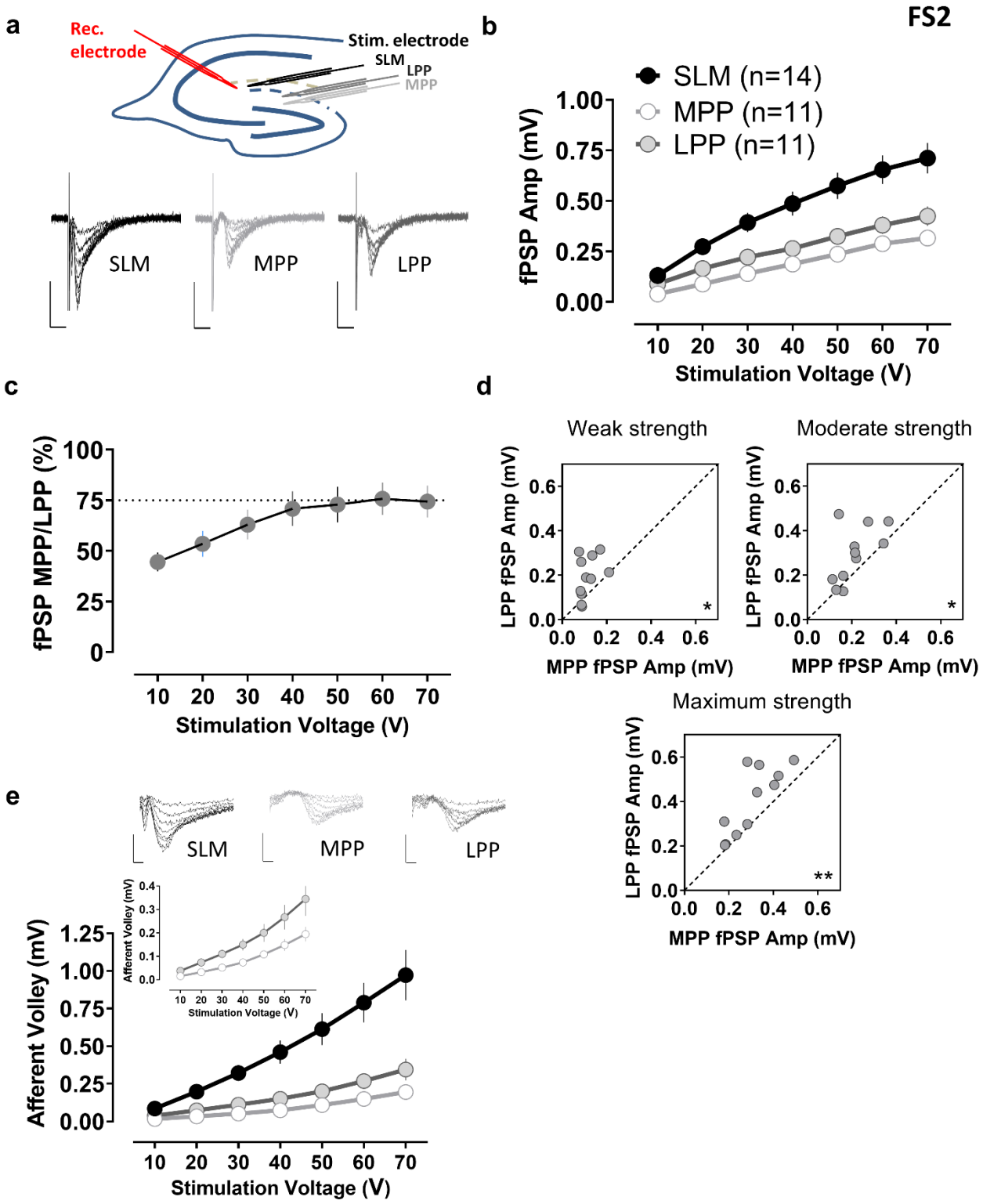

Figure S2. Electrical stimulation of the lateral perforant path evokes a larger extracellular field potential in SLM of dorsal CA2 region compared to stimulation of

medial perforant path, Related to Figure 1. a, Schematic showing the placement of stimulating electrodes as in Figure S1, while extracellularly recording from CA2 distal dendrites in SLM. The insets show representative field potentials. **b,** Electrical focal stimulation in SLM evoked a large field potential in CA2 distal dendrites (14 slices from 6 animals). The LPP-evoked response (11 slices from 5 animals) was significantly larger than the MPP-evoked response (11 slices from 5 animals) at all stimulation strengths (**c, d**). **e,** The extracellular presynaptic fiber volley in response to a stimulating pulse, which reflects the number of activated axons, was also larger in LPP than in MPP, suggesting a larger number of synaptic contacts. Scale bars: **a**: 0.5 mV/5 ms, **e**: 0.5 mV/1 ms. *: $p<0.05$, **: $p<0.01$ paired t-test.

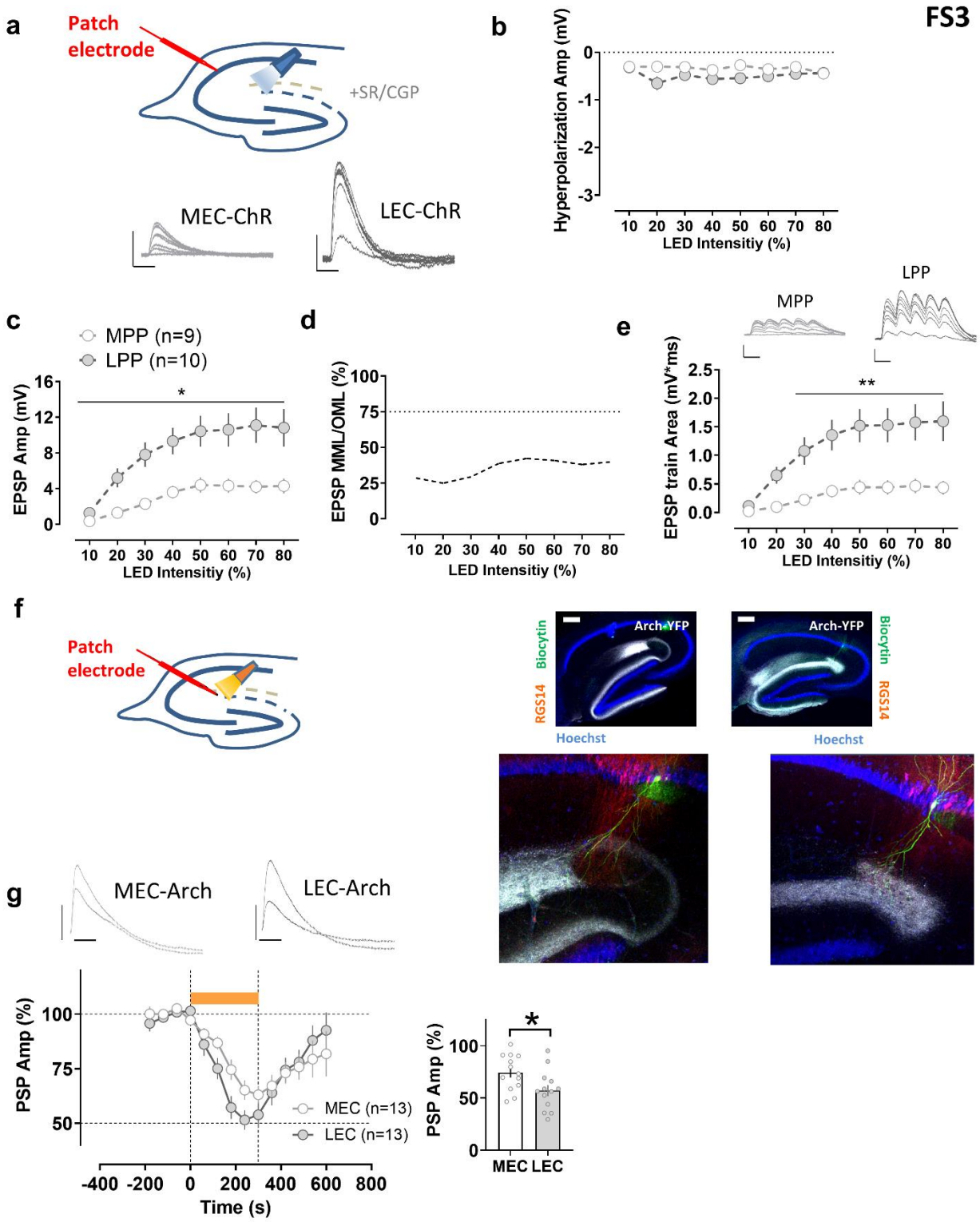

Figure S3. Optogenetic activation of lateral entorhinal cortex evokes larger excitatory postsynaptic potentials in CA2 pyramidal cells compared to activation of medial

entorhinal cortex. Optogenetic inhibition of inputs to CA2 reveals larger contribution of the lateral compared to medial entorhinal cortex, Related to Figures 1, 2 and 3. a, An AAV was injected to express ChR2 in the medial (MEC) or the lateral entorhinal cortex (LEC). All recordings were done in the presence of GABA receptor blockers to isolate the pure excitatory response (**b**). Pulses of blue light were shone on the stratum lacunosum moleculare while intracellularly recording from CA2 pyramidal neurons. **c, d,** Photostimulation of ChR2-expressing terminals in the stratum lacunosum moleculare evoked a large excitatory postsynaptic potential in CA2 pyramidal neurons for both, MEC (9 cells from 9 slices from 4 animals) and LEC (10 cells from 10 slices from 4 animals) groups. The LEC-evoked response was significantly larger than the MEC-evoked one over a range of stimulation strengths for a single light pulse and for a short train of optical stimuli (**e**). **f,** An AAV was injected in medial (MEC) or lateral entorhinal cortex (LEC) to express Arch. Illumination of the stratum lacunosum moleculare (SLM) with yellow light was used to assess the effect of optogenetic inhibition of LEC (13 cells from 13 slices from 5 animals) or MEC (13 cells from 13 slices from 6 animals) inputs on the postsynaptic depolarization in CA2 pyramidal cells evoked by electrical stimulation using an electrode in SLM. **g,** Temporal course of evoked responses. Yellow light was on for 300 s as shown in the graph. The inset shows recorded responses after 180 s of continuos illumination. Scale bars: 5 mV/25 ms and 200 µm. *: $p<0.05$, **: $p<0.01$ Holm-Sidak's post hoc test after two-way mixed-design ANOVA (in c: $F=5.762$ $p<0.0001$ for interaction Stim LED Intensity x PP M-L; in e: $F=6.885$ $p<0.0001$ for interaction Stim LED Intensity x PP M-L; in g: $F=2.675$ $p=0.0250$ for interaction Time x PP M-L).

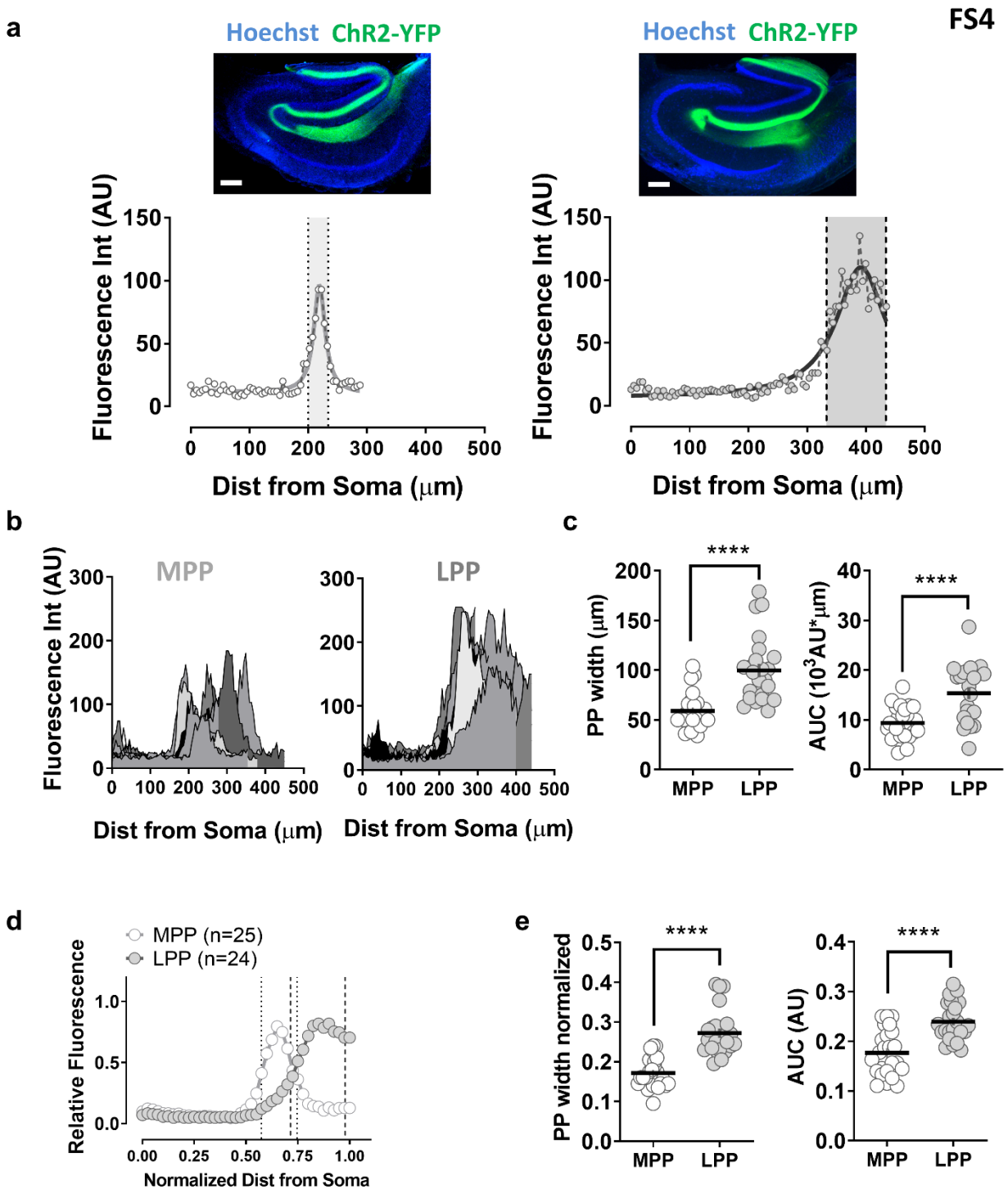

Figure S4. Lateral entorhinal cortex axons (LPP) occupy a larger area than medial entorhinal cortex ones (MPP) in the stratum lacunosum moleculare (SLM) of CA2, Related to Figure 1. a, Example images of medial, left, or lateral, right, entorhinal axons in hippocampus labelled by injecting AAV to express ChR2-YFP in MEC or LEC, respectively. Traces below the images show the intensity profiles of entorhinal axon fluorescence for

ChR2-YFP along the CA2 radial axis, from the pyramidal cell layer up to SLM. **b,** Intensity profiles of all analysed slices (MPP: 25 slices from 10 animals, LPP: 24 slices from 10 animals). **c,** LPP occupies a larger area in CA2 SLM than MPP. **d,** Intensity profiles with normalized values of fluorescence and distance. **e**, LPP has a significantly larger width in CA2 SLM than MPP. Scale bar: **a**: 200 µm. ****: $p<0.0001$ t-test.

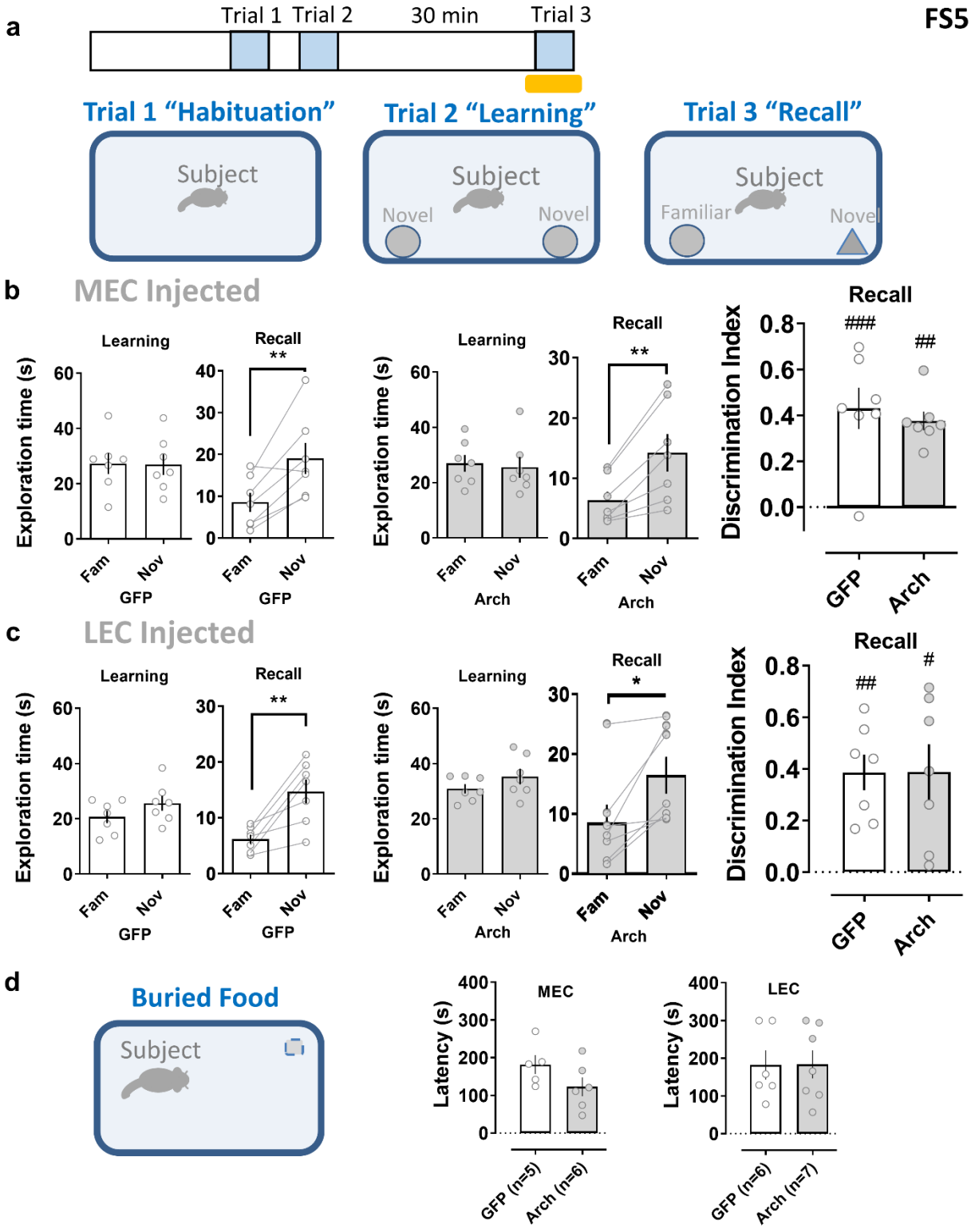

Figure S5. Disrupting the entorhinal input to dorsal CA2 does not alter novel object recognition or olfactory task performance, Related to Figures 2 and 3. a, Schema of the novel object recognition task, which is analogous to the two-choice social memory test. Shining yellow light on entorhinal cortex inputs in dorsal CA2 during the recall phase (trial 3)

did not significantly alter the performance of animals previously injected with an Arch-expressing AAV in MEC (7 animals) (**b**) or LEC (7 animals) (**c**), compared to control groups injected with GFP-expressing AAV (GFP MEC: 7 animals, GFP LEC: 7 animals). **c**, Food deprived animals searched to find a buried pellet of food. Shining yellow light on entorhinal cortex inputs in dorsal CA2 did not significantly change the performance of animals previously injected with an Arch-expressing AAV in MEC (6 animals) or LEC (7 animals), compared to GFP-expressing control groups (GFP MEC: 5 animals, GFP LEC: 6 animals). #: $p<0.05$, ##: $p<0.01$, ###: $p<0.001$ one-sample t-test against “0”. *: $p<0.05$, **: $p<0.01$ paired t-test.

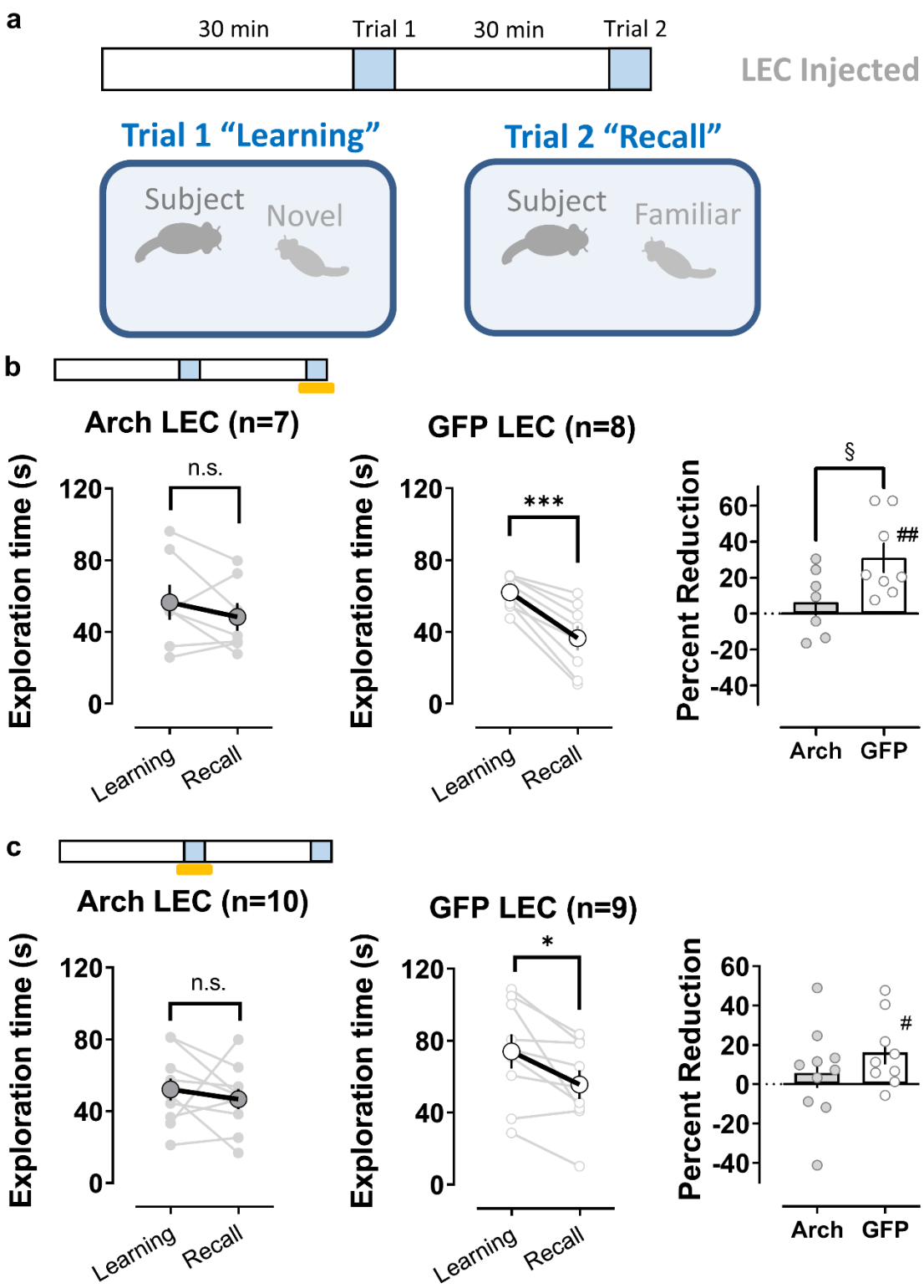

Figure S6. Disrupting the lateral entorhinal input to dorsal CA2 impairs social memory in the direct interaction task, Related to Figure 2. a, Schema of the direct interaction

social memory task. A male adult subject mouse was placed in a clean cage for a 30min habituation period. A novel juvenile male mouse was then introduced in the cage and the subject mouse was allowed to explore it for 2 min (trial 1, learning). The juvenile was removed and after a 30 min interval, the same mouse is reintroduced in trial 2. Social memory is manifest as a decrease in exploration of the now familiar juvenile in trial 2 compared to trial 1. Shining yellow light on lateral entorhinal cortex (LEC) inputs in dorsal CA2 either during the recall phase (trial 2, Arch: 7 animals, GFP: 8 animals) (**b**) or during the learning phase (trial 1, Arch: 10 animals, GFP: 9 animals) (**c**), impairs the performance of animals previously injected with an Arch-expressing AAV in LEC compared to the control group expressing GFP in LEC. §: $p<0.05$ t-test. #: $p<0.05$, ##: $p<0.01$ one-sample t-test against “0”. *: $p<0.05$,***: $p<0.001$, paired t-test.

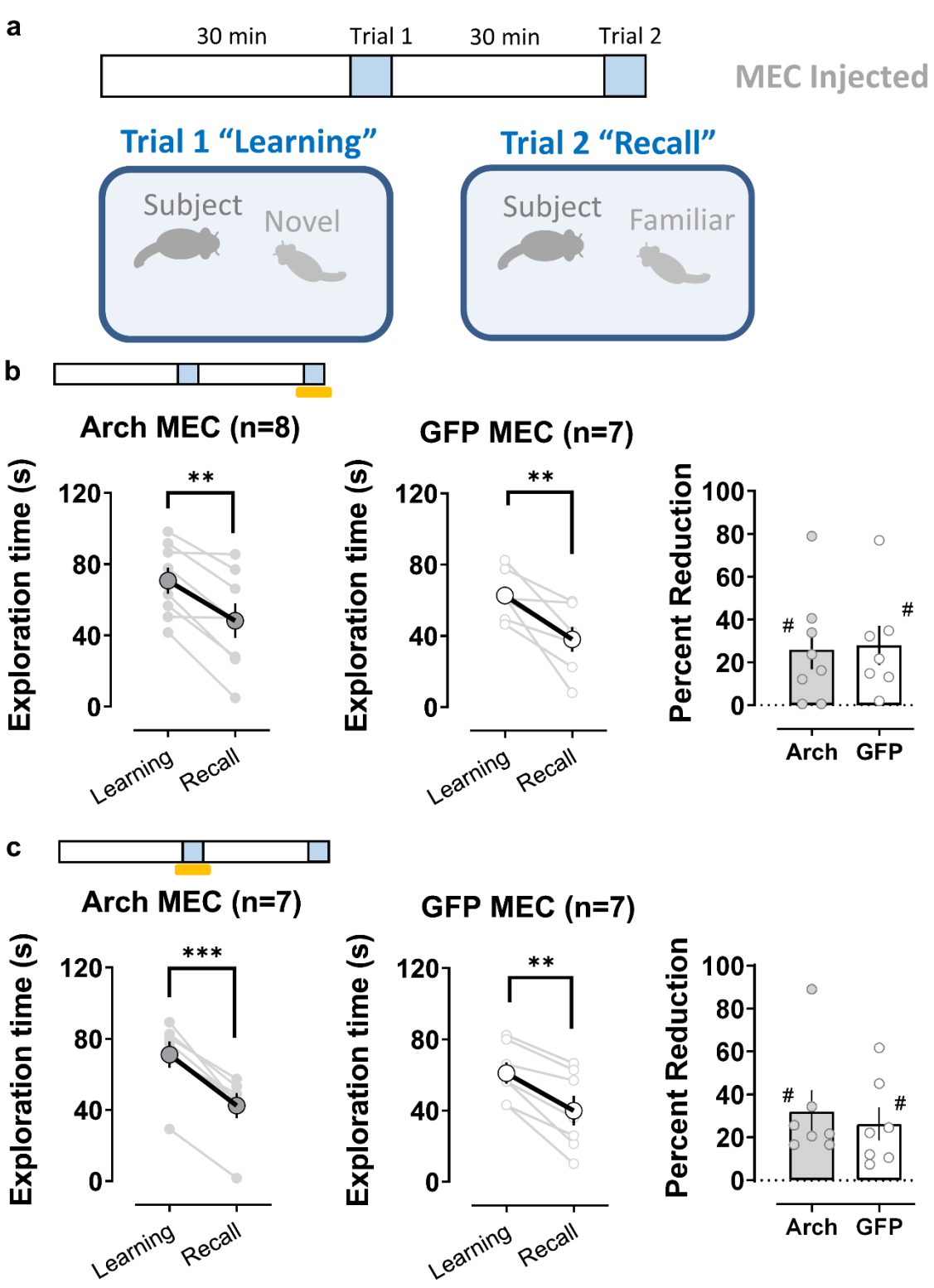

Figure S7. Disrupting the medial entorhinal input to dorsal CA2 does not influence performance in the direct interaction social memory task, Related to Figure 3. a, Schema of the direct interaction task consisting of two trials. Shining yellow light on medial

entorhinal cortex (MEC) inputs in dorsal CA2 either during the recall phase of the task (trial 2, Arch: 8 animals, GFP: 7 animals) (**b**) or during the learning phase (trial 1, Arch: 7 animals, GFP: 7 animals) (**c**), does not significantly change the performance of animals previously injected with an Arch-expressing AAV in MEC compared to a control GFP-expressing group. #: $p<0.05$, one-sample t-test against “0”. **: $p<0.01$,***: $p<0.001$, paired t-test.

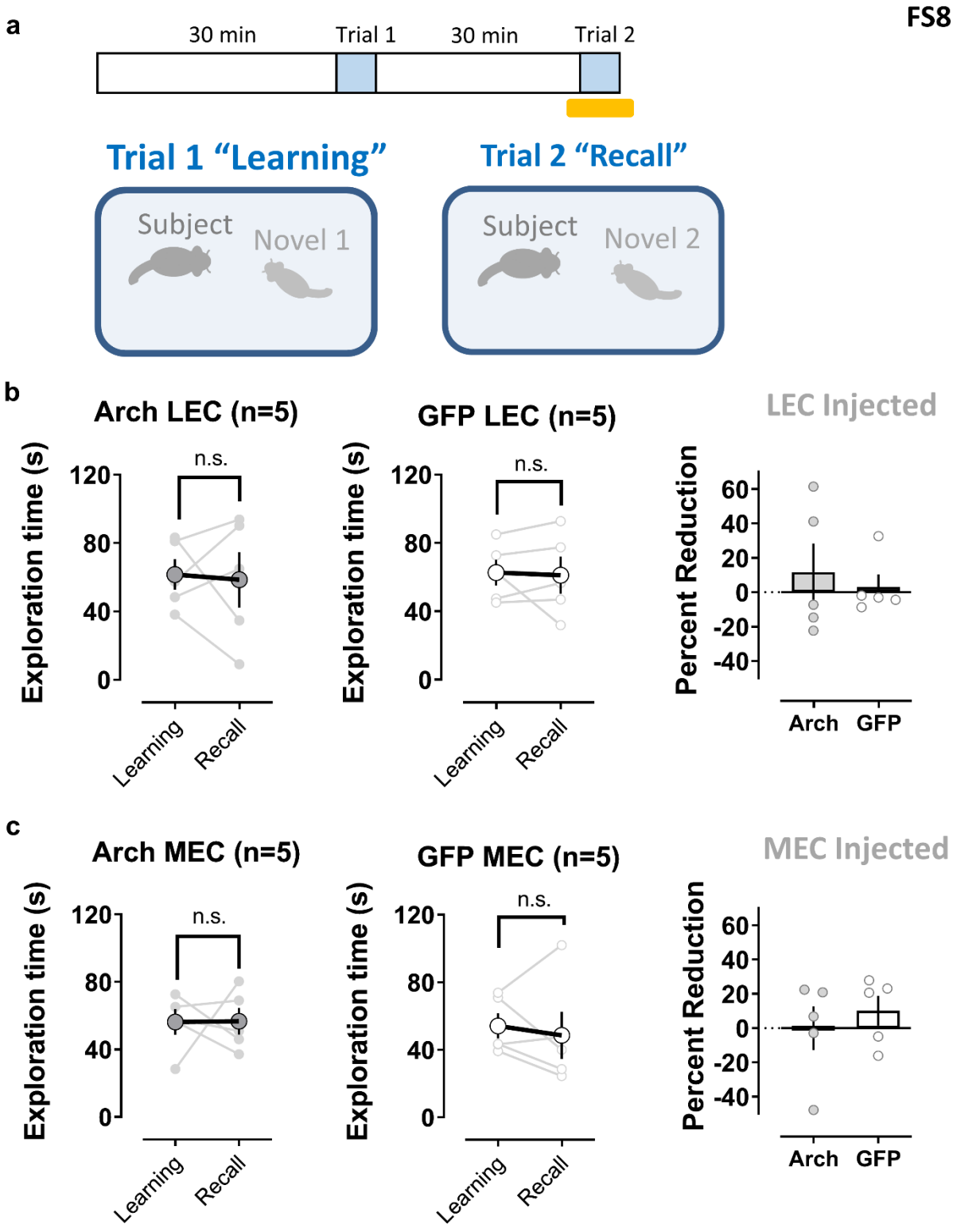

Figure S8. Decreased exploration time during the recall trial in the direct interaction task does no result from fatigue or lack of motivation for social exploration of the

subject mice, Related to Figures 2 and 3. a, Schema of the behavioral task, a variant of the direct interaction task, consisting of two trials in which a second novel juvenile male was introduced in trial 2. Mice normally show equal exploration of the two novel juveniles, indicating that the decrease in exploration when the same juvenile encountered in trial 1 is reintroduced in trial 2 reflects social memory of the now familiar mouse, rather than fatigue or lack of motivation to explore in the second trial. Shining yellow light on entorhinal cortex inputs in dorsal CA2 during the recall phase (trial 2) did not significantly change the performance of animals previously injected with an Arch-expressing AAV in LEC (5 animals) (**b**) or MEC (5 animals) (**c**), compared to GFP-expressing control groups (GFP LEC: 5 animals, GFP MEC: 5 animals).

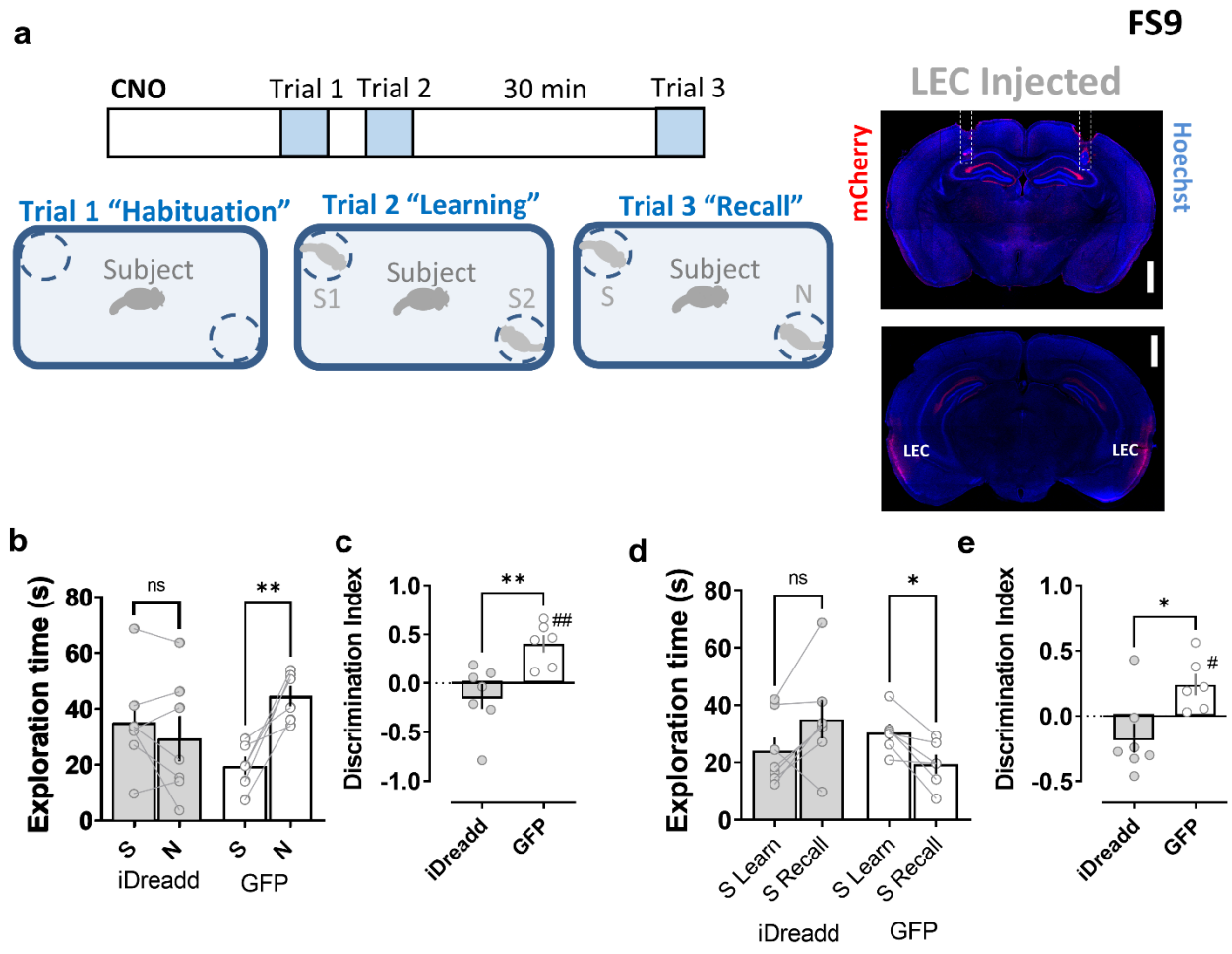

Figure S9. Pharmacogenetic silencing of the lateral entorhinal cortical input to dorsal CA2 impairs social memory, Related to Figures 2 and 4. a, Schema of the social memory task described in Figure 2. Insets show the expression of the inhibitory DREADD (iDREADD) hM4Di fused with mCherry in the lateral perforant path and the cannula location (dashed outline) in a coronal brain slice from a mouse previously injected in lateral entorhinal cortex (LEC) with an iDREADD-expressing AAV. **b-e**, Local infusion of the iDREADD agonist CNO (1 mM, 1 µl per side) in dorsal CA2 30 min before the start of the task impairs social memory performance of animals expressing iDREADD in LEC (7 animals) relative to the control group expressing GFP (6 animals). Scale bar: **a**: 1 mm. In **b**: **: p<0.01 Holm-Sidak's post hoc test after two-way mixed-design ANOVA (F=4.912 p=0.0344 for interaction Familiarity x Genotype); in **c**: **: p<0.01 t-test, ##: p<0.01 one-sample t-test against "0"; in **d**: *: p<0.05 Holm-Sidak's post hoc test after two-way mixed-design ANOVA (F=6.778 p=0.0200 for

interaction Familiar L-R x Genotype); in **e**: *: $p<0.05$ t-test, #: $p<0.05$ one-sample t-test against “0”.

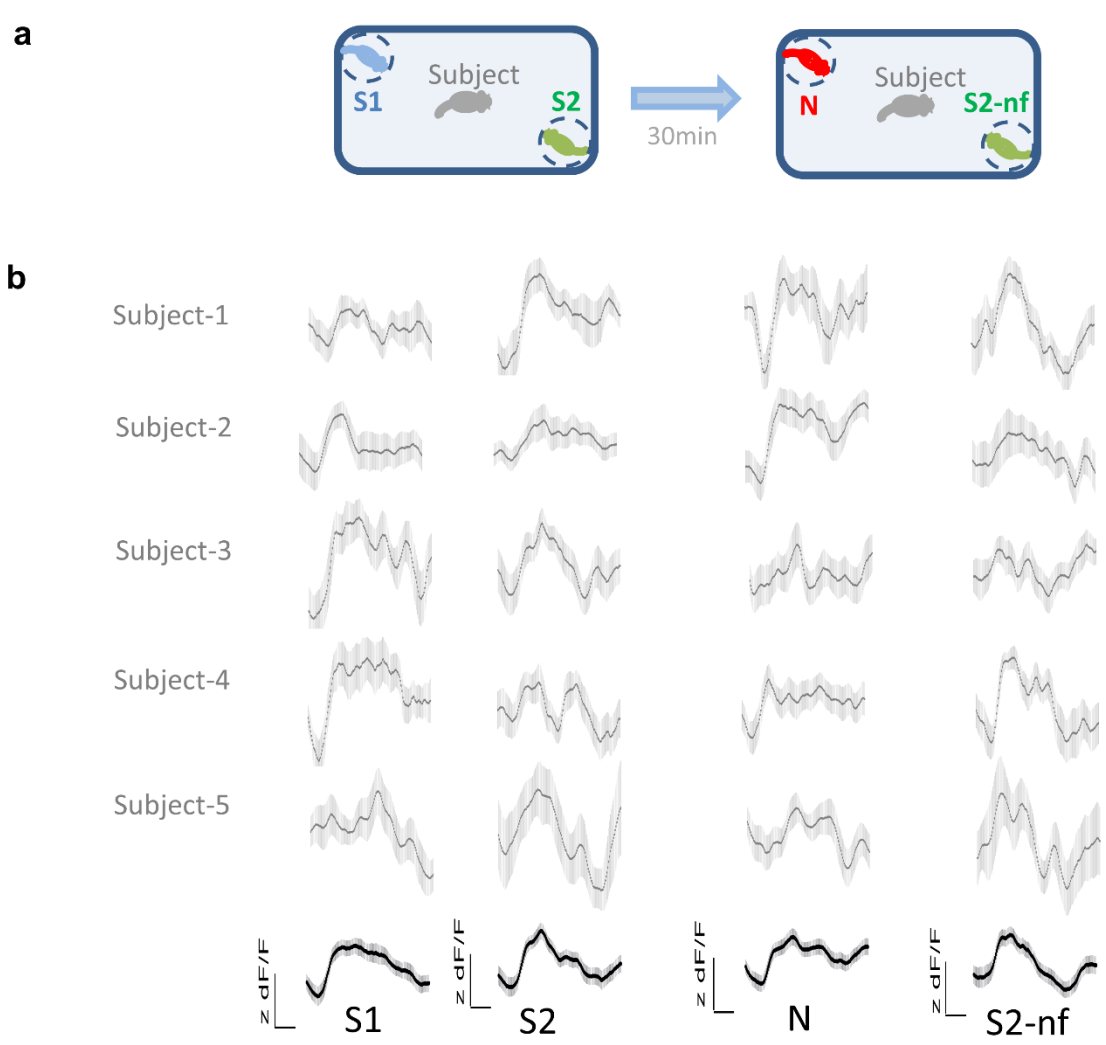

Figure S10. LEC Ca^{2+} signals from individual mice during two-choice social memory task, Related to Figure 7a-c. a, Subject mice were allowed to explore the arena with two novel mice (S1 and S2) for 5 min. The subject mouse was then removed from the arena for a 30 min intertrial interval, after which it was reintroduced to the arena and allowed to explore for another 5 min, in which one of the stimulus mice presented in learning trial (eg, S1) was replaced by a third novel mouse (N). **b**, z-scored dF/F traces from single subject animals aligned to the time of interaction. Gray traces show average fluorescence from all interaction bouts of a given type for that subject animal. Black traces show average of all animals (n=5), shown in Figure 7a.

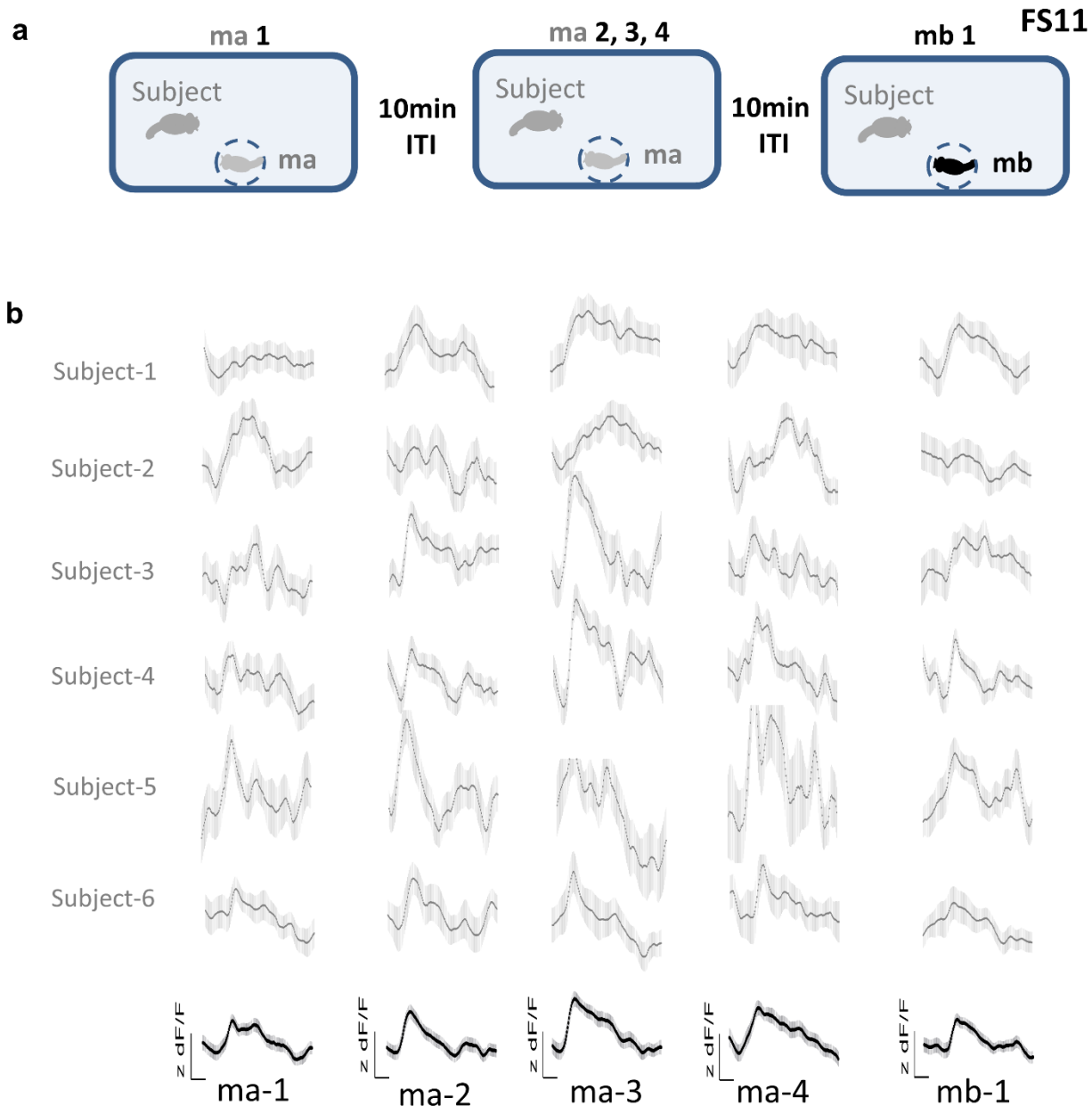

Figure S11. LEC Ca^{2+} signals from individual mice during five-trial social memory task, Related to Figure 7d-f. a, Five-trial social memory assay. **b**, z-scored dF/F traces from single subject animals aligned to the time of interaction. Gray traces show average fluorescence signals from all interaction bouts of a given type for that subject animal. Black traces show average of all animals (n=6), shown in Figure 7d.

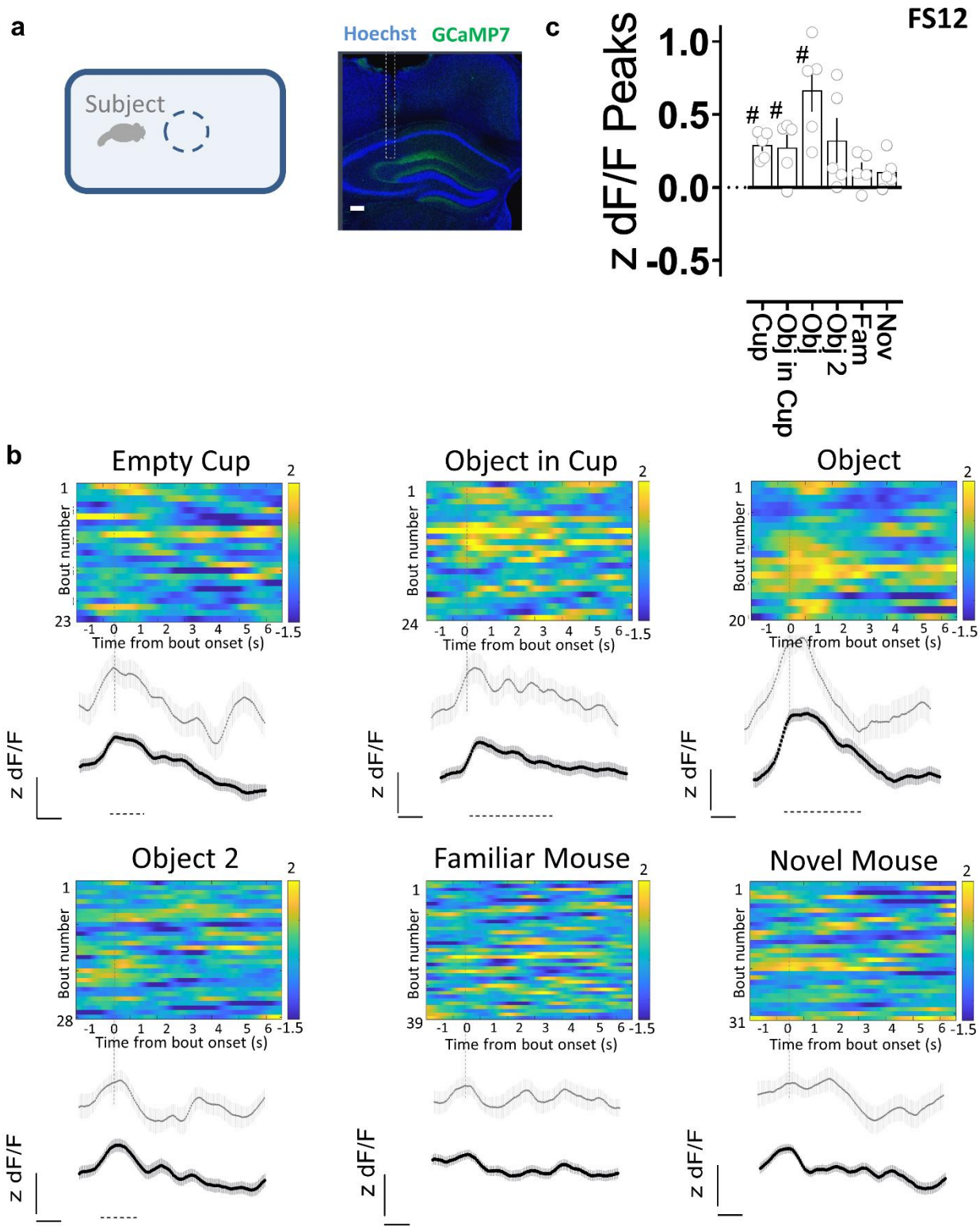

Figure S12. Activity of the medial entorhinal cortex input to dorsal CA2 does not increase during bouts of social exploration, Related to Figure 6. a, Fiber photometry

recordings of GCaMP7f fluorescence in medial entorhinal cortex (MEC) inputs to CA2 in dorsal hippocampus while an animal explores indicated items in an open arena. Coronal section of the hippocampus showing the expression of GCaMP7f and the optical fiber location (dashed outline) in mice previously injected with AAV in MEC. **b**, Ca2+ signals in MEC inputs to CA2 during bouts of social or object exploration. Color-coded z-scored dF/F traces from a single animal aligned to the time of interaction. Gray traces show average fluorescence from all interaction bouts of a given type for that animal. Black traces show average of all animals (n=5). Dashed line below the traces indicates the time window with a significant difference with respect to baseline. **c**, Mean peak Ca2+ signals during indicated interactions relative to baseline. Each symbol from a different animal. #: $p<0.05$ one-sample t-test against “0”.